



Polynomial Splines and their Tensor Products in Extended Linear Modeling

Charles J. Stone; Mark H. Hansen; Charles Kooperberg; Young K. Truong

The Annals of Statistics, Vol. 25, No. 4. (Aug., 1997), pp. 1371-1425.

Stable URL:

<http://links.jstor.org/sici?sici=0090-5364%28199708%2925%3A4%3C1371%3APSATTP%3E2.0.CO%3B2-S>

The Annals of Statistics is currently published by Institute of Mathematical Statistics.

Your use of the JSTOR archive indicates your acceptance of JSTOR's Terms and Conditions of Use, available at <http://www.jstor.org/about/terms.html>. JSTOR's Terms and Conditions of Use provides, in part, that unless you have obtained prior permission, you may not download an entire issue of a journal or multiple copies of articles, and you may use content in the JSTOR archive only for your personal, non-commercial use.

Please contact the publisher regarding any further use of this work. Publisher contact information may be obtained at <http://www.jstor.org/journals/ims.html>.

Each copy of any part of a JSTOR transmission must contain the same copyright notice that appears on the screen or printed page of such transmission.

JSTOR is an independent not-for-profit organization dedicated to and preserving a digital archive of scholarly journals. For more information regarding JSTOR, please contact support@jstor.org.

1994 WALD MEMORIAL LECTURE

POLYNOMIAL SPLINES AND THEIR TENSOR PRODUCTS IN EXTENDED LINEAR MODELING

BY CHARLES J. STONE,¹ MARK H. HANSEN, CHARLES KOOPERBERG²
AND YOUNG K. TRUONG³

*University of California, Berkeley, Bell Laboratories,
University of Washington and University of North Carolina, Chapel Hill*

Analysis of variance type models are considered for a regression function or for the logarithm of a probability function, conditional probability function, density function, conditional density function, hazard function, conditional hazard function or spectral density function. Polynomial splines are used to model the main effects, and their tensor products are used to model any interaction components that are included. In the special context of survival analysis, the baseline hazard function is modeled and nonproportionality is allowed. In general, the theory involves the L_2 rate of convergence for the fitted model and its components. The methodology involves least squares and maximum likelihood estimation, stepwise addition of basis functions using Rao statistics, stepwise deletion using Wald statistics and model selection using the Bayesian information criterion, cross-validation or an independent test set. Publicly available software, written in C and interfaced to S/S-PLUS, is used to apply this methodology to real data.

1. Introduction. The last two decades have witnessed an incredible change in the focus of statistical theory and methodology. Fueled in part by the explosion of available computer power, highly adaptive, functional procedures are now essential tools for modern data analysis. While freed from the rigid assumptions implicit in classical parametric models, the statistician is now expected to select not only the important variables in a model, but also the functional form of the dependence on these variables. To be practically successful, any new adaptive procedure must inevitably strike a balance between flexibility and the haunting “curse of dimensionality.” It is in this capacity that statistical theory is critical to the success of emerging methodologies. Polynomial splines and their tensor products offer the flexibility required for modern data analysis, and when used in concert with low-dimensional analysis of variance (ANOVA) decompositions, effectively tame the curse of dimensionality.

Received August 1995; revised December 1996.

¹Research supported in part by NSF Grants DMS-92-04247 and DMS-95-04463.

²Research supported in part by NSF Grant DMS-94-03371 and NIH Grant CA61937.

³Research supported in part by NSF Grant DMS-94-03800 and NIH Grant CA61937.

AMS 1991 subject classifications. Primary 62G07; secondary 62J12.

Key words and phrases. ANOVA, density estimation, generalized additive models, generalized linear models, least squares, logistic regression, maximum likelihood, model selection, multiple classification, nonparametric regression, optimal rates of convergence, proportional hazards model, spectral estimation, survival analysis.

In the pages that follow, we will alternate between a discussion of the practical implementation of this methodology and a very broad theoretical investigation into the properties of this approach in the context of *extended linear models*. We have coined this term because our theoretical results apply to a group of estimation problems that subsumes the classical exponential family regression models [see McCullagh and Nelder (1989)]. While our initial motivation for introducing this family was to achieve a theoretical synthesis, we found that this framework also allows us to entertain a fairly general treatment of the associated methodology. Throughout our presentation, however, we maintain a distinction between the nonadaptive procedures that we can treat theoretically and the adaptive methodologies that we have implemented for density estimation, hazard regression, polychotomous regression and spectral density estimation. In this presentation, we concentrate on theoretical and methodological innovations developed through many collaborations involving various subsets of the authors of the present paper.

In Section 2, we define the notion of an extended linear model and use this framework simultaneously to discuss the L_2 rate of convergence for the nonadaptive version of our procedures in a variety of important statistical settings, while in Section 3, we translate these promising theoretical results into practically useful, adaptive methodology. Ultimately, however, the true measure of any statistical procedure is its performance on real data. In Sections 4–9 we focus on a number of specific modeling problems for which our approach has yielded successful data analysis tools. In each case, an S/S-PLUS implementation is (or will soon be made) publicly available so that the “true measure” of these procedures can be judged on the wealth of data that exist beyond the (necessarily narrow) confines of our examples. Logspline density estimation was our first attempt at an adaptive spline-based methodology, and in Section 4 we present the latest version of this procedure, LOGSPLINE. In Section 5 we describe our own version of MARS [Friedman (1991)] as a routine to handle regression problems involving many predictors. The motivation for reworking this routine stems from an application of linear splines to polychotomous regression, known as POLYCLASS, which is described in Section 6. In order to relax the proportionality and linearity assumptions in classical survival analysis, we have developed spline routines for hazard estimation with flexible tails (HEFT) and hazard regression (HARE). These are the subject of Section 7. Spectral density estimation is another area in which our adaptive methodology can easily capture all the relevant features of a given time series, and in Section 8 we discuss LSPEC, an implementation of this approach. We end the paper with a discussion of Triogram models, a methodology for bivariate function estimation through the use of splines defined over adaptively determined triangulations.

2. Extended linear models: theory.

Notation. Consider a \mathscr{W} -valued random variable \mathbf{W} , where \mathscr{W} is an arbitrary set. Let $\mathscr{U} = \mathscr{U}_1 \times \cdots \times \mathscr{U}_M$ be a Cartesian product of compact intervals,

each having positive length. Let K be a positive integer. Consider a vector-valued function $h = (h_1, \dots, h_K)$ on \mathcal{U} whose constituents h_1, \dots, h_K are real-valued functions on \mathcal{U} . Let $l(h, \mathbf{W})$ be a (not necessarily true) log-likelihood and let $\Lambda(h) = E[l(h, \mathbf{W})]$ be the corresponding expected log-likelihood. There may be some mild restrictions on h for the log-likelihood to be defined. We assume that, subject to such restrictions, there is an essentially unique function $\phi = (\phi_1, \dots, \phi_K)$ that maximizes the expected log-likelihood. (Here two functions on \mathcal{U} are essentially equal if they differ only on a subset of \mathcal{U} having Lebesgue measure zero.)

Let H be a linear space of real-valued functions on \mathcal{U} , let H^K denote the space of functions of the form $h = (h_1, \dots, h_K)$, where the constituents h_1, \dots, h_K of h range over H , and consider the log-likelihood function $l(h, \mathbf{W})$, $h \in H^K$. We refer to any particular setup of this form as an *extended linear model*. The expected log-likelihood function is given by $\Lambda(h)$, $h \in H^K$. The model is said to be concave if $l(h, \mathbf{w})$ is a concave function of h for each $\mathbf{w} \in \mathcal{W}$ and $\Lambda(h)$ is a strictly concave function of h when restricted to those functions $h \in H^K$ such that $\Lambda(h) > -\infty$. Typically, when the model is concave, there is an essentially unique function $\phi^* = (\phi_1^*, \dots, \phi_K^*) \in H^K$ that maximizes the expected log-likelihood over H^K . It follows from the information inequality that if $\phi \in H^K$, then $\phi^* = \phi$.

In order to define ANOVA decompositions of the constituents of ϕ^* , we first need to define corresponding theoretical inner products and norms. To this end, let ψ be an absolutely continuous measure on \mathcal{U} having a density function that is bounded away from zero and infinity on \mathcal{U} . Given square-integrable, real-valued functions h_1 and h_2 on \mathcal{U} , their theoretical inner product is defined by $\langle h_1, h_2 \rangle = \int_{\mathcal{U}} h_1 h_2 d\psi$. Given such a function h , its theoretical norm is defined by $\|h\|^2 = \langle h, h \rangle = \int_{\mathcal{U}} h^2 d\psi$. Conversely, if $\|\cdot\|$ is defined directly, then ψ is defined implicitly by the formula $\psi(A) = \|\text{ind}_A\|^2$, where ind_A is the indicator function of A , which equals 1 on A and 0 on A^c .

Let $\mathbf{W}_1, \dots, \mathbf{W}_n$ be a random sample of size n from the distribution of \mathbf{W} . The log-likelihood function corresponding to this random sample is given by $l(h) = \sum_i l(h, \mathbf{W}_i)$. Let $G = G_n$ be a finite-dimensional subspace of H and let $G^K = G_n^K$ denote the corresponding subspace of H^K . (Note that if $K = 1$, then $H^K = H$ and $G^K = G$.) Under the assumptions of a concave extended linear model and reasonable additional conditions, except on an event whose probability tends to zero as $n \rightarrow \infty$, there is a unique maximum likelihood estimate $\hat{\phi}$ in G^K of ϕ^* ; that is, a unique function $\hat{\phi} = (\hat{\phi}_1, \dots, \hat{\phi}_K)$ in G^K that maximizes the log-likelihood function over G^K .

In order to define ANOVA decompositions of the constituents of $\hat{\phi}$, we need to define corresponding empirical inner products and norms. For $n \geq 1$, let ψ_n be an empirical product measure on \mathcal{U} that is a transform (measurable function) of the random sample $\mathbf{W}_1, \dots, \mathbf{W}_n$. (Roughly speaking, ψ_n should approach ψ as $n \rightarrow \infty$.) Given real-valued functions h_1 and h_2 on \mathcal{U} , their empirical inner product is defined by $\langle h_1, h_2 \rangle_n = \int_{\mathcal{U}} h_1 h_2 d\psi_n$. Given such a function h , its empirical norm is defined by $\|h\|_n^2 = \int_{\mathcal{U}} h^2 d\psi_n$. The space G is

said to be *identifiable* if the only function $g \in G$ such that $\|g\|_n = 0$ is given by $g = 0$. Under reasonable conditions, G is identifiable except on an event whose probability tends to zero as $n \rightarrow \infty$.

Many statistical problems of theoretical and practical importance can effectively be treated within the framework of concave extended linear models. Most of the investigations in this framework have involved a \mathcal{U} -valued random variable \mathbf{U} that is a transform of \mathbf{W} . Let $\mathbf{U}_1, \dots, \mathbf{U}_n$ be the corresponding transforms of $\mathbf{W}_1, \dots, \mathbf{W}_n$, respectively. Here, we typically let ψ be the distribution of \mathbf{U} and ψ_n the empirical distribution of $\mathbf{U}_1, \dots, \mathbf{U}_n$.

EXAMPLES.

Regression. Consider a random pair (\mathbf{X}, Y) , where \mathbf{X} is \mathcal{X} -valued and Y is real-valued and has finite second moment. Set $l(h, \mathbf{X}, Y) = -[Y - h(\mathbf{X})]^2$. Then we get a concave extended linear model with $\mathbf{W} = (\mathbf{X}, Y)$, $\mathbf{U} = \mathbf{X}$ and $K = 1$. If H is the space of all functions h on \mathcal{X} with $E[h^2(\mathbf{X})] < \infty$, then ϕ is the regression function of Y on \mathbf{X} . More generally, if H is a Hilbert space of such functions h , then ϕ^* is the best approximation in H to the regression function, where "best" means minimizing the mean squared error $E\{[Y - h(\mathbf{X})]^2\}$ in predicting Y by $h(\mathbf{X})$. Here maximum likelihood estimation in G coincides with least squares estimation.

Generalized regression. Suppose now that, for each $\mathbf{x} \in \mathcal{X}$, the conditional distribution of Y given that $\mathbf{X} = \mathbf{x}$ belongs to a fixed exponential family of distributions on \mathbb{R} of the form $\exp[B(\theta)y - C(\theta)]\rho(dy)$, where the parameter θ ranges over \mathbb{R} . Here ρ is a nonzero measure on \mathbb{R} that is not concentrated at a single point and $\int_{\mathbb{R}} \exp[B(\theta)y - C(\theta)]\rho(dy) = 1$ for $\theta \in \mathbb{R}$. The function $B(\cdot)$ is required to be twice continuously differentiable and its first derivative $B'(\cdot)$ is required to be strictly positive on \mathbb{R} . It is required that there be a subinterval S of \mathbb{R} such that ρ is concentrated on S and $B''(\theta)y - C'(\theta) < 0$ for $\theta \in \mathbb{R}$ and $y \in S$. If S is bounded, it is required that it contain at least one of its endpoints. Let h be a candidate for the dependence of θ on \mathbf{x} . The corresponding (conditional) log-likelihood is given by $l(h, \mathbf{X}, Y) = B(h(\mathbf{X}))Y - C(h(\mathbf{X}))$. This has the form of a concave extended linear model with $\mathbf{W} = (\mathbf{X}, Y)$, $\mathbf{U} = \mathbf{X}$ and $K = 1$. As special cases, we get logistic regression, probit regression and Poisson regression models.

Polytomous regression. Let Y be a qualitative random variable having $K + 1$ possible values. Without loss of generality, we can think of this random variable as ranging over $\mathcal{Y} = \{1, \dots, K + 1\}$. Suppose that $P(Y = k | \mathbf{X} = \mathbf{x}) > 0$ for $\mathbf{x} \in \mathcal{X}$ and $k \in \mathcal{Y}$. For $1 \leq k \leq K$, let h_k be a candidate for the function

$$\log \frac{P(Y = k | \mathbf{X} = \mathbf{x})}{P(Y = K + 1 | \mathbf{X} = \mathbf{x})}.$$

The corresponding log-likelihood is given by

$$l(h, \mathbf{X}, Y) = h_1(\mathbf{X})I_1(Y) + \dots + h_K(\mathbf{X})I_K(Y) \\ - \log(1 + \exp h_1(\mathbf{X}) + \dots + \exp h_K(\mathbf{X})),$$

where $I_k(Y)$ equals 1 or 0 according as $Y = k$ or $Y \neq k$ and $h = (h_1, \dots, h_K)$. This setup has the form of a concave extended linear model with $\mathbf{W} = (\mathbf{X}, Y)$ and $\mathbf{U} = \mathbf{X}$.

Density estimation. Let \mathbf{Y} have an unknown positive density function on \mathcal{Y} . We can write its log-density function in the form $\phi - C(\phi)$, where $C(\phi) = \log \int \exp h(\mathbf{y}) d\mathbf{y}$. The corresponding log-likelihood function is given by $l(h, \mathbf{Y}) = h(\mathbf{Y}) - C(h)$. This setup has the form of a concave extended linear model with $\mathbf{W} = \mathbf{U} = \mathbf{Y}$ and $K = 1$ provided that, for identifiability, we impose a restriction on the functions $h \in H$ such as $E[h(\mathbf{U}) = 0]$ and we impose a similar condition on the functions in G .

Hazard regression. Consider a positive survival time T , a positive censoring time C , the observed time $\min(T, C)$ and an \mathcal{X} -valued random vector \mathbf{X} of covariates. Let $\delta = \text{ind}(T \leq C)$ be the indicator random variable that equals 1 or 0 according as $T \leq C$ (T is uncensored) or $T > C$ (T is censored) and write $\min(T, C)$ as $T \wedge C$. Suppose T and C are conditionally independent given \mathbf{X} . For theoretical purposes, it is supposed that $P(C \leq \tau) = 1$, where τ is a known positive constant. Set $\mathbf{W} = (\mathbf{X}, T \wedge C, \delta)$ and $\mathbf{U} = (\mathbf{X}, T \wedge C)$. Let $\phi(\mathbf{x}, t) = \log f(t|\mathbf{x})/[1 - F(t|\mathbf{x})]$, $t > 0$, denote the logarithm of the conditional hazard function, where $f(t|\mathbf{x})$ and $F(t|\mathbf{x})$ are the conditional density and distribution functions, respectively, of T given that $\mathbf{X} = \mathbf{x}$. Since the likelihood equals $f(T \wedge C|\mathbf{X})$ for an uncensored case and $1 - F(T \wedge C|\mathbf{X})$ for a censored case, it can be written as

$$\begin{aligned} & [f(T \wedge C|\mathbf{X})]^\delta [1 - F(T \wedge C|\mathbf{X})]^{1-\delta} \\ &= \left(\frac{f(T \wedge C|\mathbf{X})}{1 - F(T \wedge C|\mathbf{X})} \right)^\delta [1 - F(T \wedge C|\mathbf{X})] \\ &= [\exp \phi(\mathbf{X}, T \wedge C)]^\delta \exp \left(- \int_0^{T \wedge C} \exp \phi(\mathbf{X}, t) dt \right). \end{aligned}$$

Thus the log-likelihood function is given by

$$l(h, \mathbf{W}) = \delta h(\mathbf{X}, T \wedge C) - \int_0^{T \wedge C} \exp h(\mathbf{X}, t) dt.$$

This setup has the form of a concave extended linear model with $K = 1$. Here the theoretical inner product is given by

$$\langle h_1, h_2 \rangle = E \int_0^{T \wedge C} h_1(t, \mathbf{X}) h_2(t, \mathbf{X}) dt,$$

which defines ψ implicitly; the corresponding empirical inner product $\langle \cdot, \cdot \rangle_n$ and empirical measure ψ_n are defined in the obvious manner.

ANOVA decompositions and convergence rates. In the theoretical development of extended linear models, ANOVA decompositions of ϕ^* , $\hat{\phi}$, and their constituents play important roles. For a simple illustration of such decompositions, consider a regression or generalized regression context with $M = 2$

and let H be the space of all square-integrable functions on \mathcal{U} . Then ϕ can be written as

$$(2.1) \quad \phi(x_1, x_2) = \phi_0 + \phi_1(x_1) + \phi_2(x_2) + \phi_{12}(x_1, x_2).$$

Here ϕ_0 is the constant component, ϕ_1 and ϕ_2 are the main effect components and ϕ_{12} is the two-factor interaction component. It is required that each component be theoretically orthogonal to all choices of the corresponding lower-order components; that is, ϕ_1, ϕ_2 and ϕ_{12} are each theoretically orthogonal to 1, and ϕ_{12} is orthogonal to all choices of ϕ_1 and ϕ_2 . The maximum number d of factors in any component of the model is given by $d = 2$. Since $d = M$, the model is saturated.

Given a random sample, consider an estimate

$$(2.2) \quad \hat{\phi}(x_1, x_2) = \hat{\phi}_0 + \hat{\phi}_1(x_1) + \hat{\phi}_2(x_2) + \hat{\phi}_{12}(x_1, x_2),$$

where each component is empirically orthogonal to all choices of the corresponding lower-order components. The right-hand sides of (2.1) and (2.2) are referred to as the ANOVA decompositions of ϕ and $\hat{\phi}$, respectively.

Removing the interaction component, we get the additive ($d = 1$), unsaturated approximation

$$\phi^*(x_1, x_2) = \phi_0^* + \phi_1^*(x_1) + \phi_2^*(x_2)$$

to ϕ and the corresponding estimate

$$\hat{\phi}(x_1, x_2) = \hat{\phi}_0 + \hat{\phi}_1(x_1) + \hat{\phi}_2(x_2).$$

In general, given a subset s of $\{1, \dots, M\}$, let H_s denote the space of square-integrable, real-valued functions on \mathcal{U} that depend only on the variables u_m , $m \in s$. (The space H_\emptyset corresponding to the empty set \emptyset is the space of constant functions.) Let \mathcal{S} denote a hierarchical collection of subsets of $\{1, \dots, M\}$, where hierarchical means that if s is a member of \mathcal{S} and r is a subset of s , then r is a member of \mathcal{S} . Let H now denote the space of functions on \mathcal{U} of the form $\sum_{s \in \mathcal{S}} h_s$, where $h_s \in H_s$ for $s \in \mathcal{S}$. Let d denote the maximum cardinality of the sets $s \in \mathcal{S}$. We refer to this setup as being *saturated* if $d = M$ and *unsaturated* if $d < M$. If $d = 1$, then the functions in H are additive functions of the individual coordinates.

Let $h \perp H_r$ mean that $\langle h, h_r \rangle = 0$ for $h_r \in H_r$. Every function $h \in H$ can then be written in an essentially unique manner as $h = \sum_{s \in \mathcal{S}} h_s$, where, for $s \in \mathcal{S}$, $h_s \in H_s$ and $h_s \perp H_r$ for every proper subset r of s . We refer to h_s , $s \in \mathcal{S}$, as the *components* of the ANOVA decomposition of h . In particular, let ϕ_{ks}^* , $s \in \mathcal{S}$, denote the components of the ANOVA decomposition of ϕ_k^* . Also, set $\phi_s^* = (\phi_{1s}^*, \dots, \phi_{Ks}^*)$ for $s \in \mathcal{S}$.

For $1 \leq m \leq M$, let G_m denote a finite-dimensional space of functions on \mathcal{U}_m containing the constant functions. Given a subset s of $\{1, \dots, M\}$, let G_s denote the tensor product of the spaces G_m , $m \in s$, which is the space spanned by functions on \mathcal{U} of the form $\prod_{m \in s} g_m(u_m)$ as g_m ranges over G_m for $m \in s$. Observe that $G_r \subset G_s$ for $r \subset s$. Let G denote the space of functions on \mathcal{U} of the form $\sum_{s \in \mathcal{S}} g_s$, where $g_s \in G_s$ for $s \in \mathcal{S}$.

Let $g \perp_n G_r$ mean that $\langle g, g_r \rangle_n = 0$ for $g_r \in G_r$. If G is identifiable, then every function $g \in G$ can be written uniquely as $g = \sum_{s \in \mathcal{S}} g_s$, where, for $s \in \mathcal{S}$, $g_s \in G_s$ and $g_s \perp_n G_r$ for every proper subset r of s . We refer to g_s , $s \in \mathcal{S}$, as the components of the ANOVA decomposition of g . In particular, let $\hat{\phi}_{ks}$, $s \in \mathcal{S}$, denote the components of the ANOVA decomposition of $\hat{\phi}_k$. Also, set $\hat{\phi}_s = (\hat{\phi}_{1s}, \dots, \hat{\phi}_{Ks})$ for $s \in \mathcal{S}$.

We now restrict attention to spaces G_m of polynomial splines. For theoretical simplicity, for $1 \leq m \leq M$, let Δ_m be a partition of \mathcal{U}_m into disjoint intervals having common length a . By a piecewise polynomial of degree q on \mathcal{U}_m , we mean a function g on \mathcal{U}_m such that the restriction of g to each $\delta \in \Delta_m$ is a polynomial of degree q . Let G_m be a linear space of splines on \mathcal{U}_m —that is, piecewise polynomials of degree q on \mathcal{U}_m subject to specified smoothness constraints, typically that of being $(q - 1)$ -times continuously differentiable on \mathcal{U}_m .

Given a real-valued function h on \mathcal{U} , let $\|h\|_\infty$ denote the supremum of $|h|$ on \mathcal{U} . Given a vector-valued function $h = (h_1, \dots, h_K)$ on \mathcal{U} , set $\|h\|_\infty = \max(\|h_1\|_\infty, \dots, \|h_K\|_\infty)$ and $\|h\|^2 = \|h_1\|^2 + \dots + \|h_K\|^2$.

Next we consider the rates of convergence that can theoretically be established for the estimate $\hat{\phi}$ of ϕ^* and for the corresponding estimates $\hat{\phi}_s$ of the components ϕ_s^* of ϕ^* . Let $s \in \mathcal{S}$. Under various conditions on the spaces G_m , $m \in s$,

$$\inf_{g \in G_s} \|g - \phi_{ks}^*\|_\infty = O(a^p), \quad 1 \leq k \leq K \text{ and } s \in \mathcal{S},$$

with p being a suitably defined measure of smoothness of the constituents of ϕ^* . Under various reasonable additional conditions,

$$\|\hat{\phi}_s - \phi_s^*\|^2 = O_P\left(a^{2p} + \frac{1}{na^d}\right), \quad s \in \mathcal{S},$$

and

$$\|\hat{\phi} - \phi^*\|^2 = O_P\left(a^{2p} + \frac{1}{na^d}\right).$$

Thus, by optimally choosing $a \sim n^{-1/(2p+d)}$, we get the rate of convergence given by

$$(2.3) \quad \|\hat{\phi}_s - \phi_s^*\| = O_P(n^{-p/(2p+d)}), \quad s \in \mathcal{S},$$

and

$$(2.4) \quad \|\hat{\phi} - \phi^*\| = O_P(n^{-p/(2p+d)}).$$

In particular, by considering additive models ($d = 1$) or by allowing interactions involving only two factors ($d = 2$), we can get faster rates of convergence than by choosing $d = M$ and thereby ameliorate the “curse of dimensionality.”

Hansen (1994) introduced the class of extended linear models and obtained the corresponding L_2 rates of convergence. The various cases of this theory that have previously been treated are as follows: regression in Stone (1985,

1994); generalized regression in Stone (1986, 1994), density estimation in Stone (1990, 1994); conditional density estimation in Stone (1991, 1994) and Hansen (1994); hazard regression in Kooperberg, Stone and Truong (1995b); and spectral density estimation in Kooperberg, Stone and Truong (1995d).

3. Extended linear models: adaptive methodology. In practice, it seems best to select G in an adaptive manner. Let J be the dimension of G , let B_1, \dots, B_J be a basis of this space and write a candidate $g = (g_1, \dots, g_K)$ for the maximum likelihood estimate $\hat{\phi}$ in G of ϕ^* as $g_k = \sum_j \beta_{jk} B_j$ for $1 \leq k \leq K$. Let β be the (suitably) ordered JK -tuple $(\beta_{jk})_{1 \leq j \leq J, 1 \leq k \leq K}$. Then the log-likelihood function based on the sample data can be written as $l(\beta)$, $\beta \in \mathcal{B}$. Assume that this log-likelihood function is twice continuously differentiable, and let $\nabla l(\beta)$ and $\mathbf{H}(\beta)$ denote its gradient and Hessian matrix, respectively, at β .

The quadratic approximation Q to the log-likelihood function about $\beta_0 \in \mathcal{B}$ is given by

$$(3.1) \quad Q(\beta) = l(\beta_0) + [\nabla l(\beta_0)]^T (\beta - \beta_0) + \frac{1}{2} (\beta - \beta_0)^T \mathbf{H}(\beta_0) (\beta - \beta_0).$$

Suppose $\mathbf{H}(\beta_0)$ is negative definite or, equivalently, that $\mathbf{I}(\beta_0) = -\mathbf{H}(\beta_0)$ is positive definite. Then Q is uniquely maximized at

$$(3.2) \quad \beta_1 = \beta_0 + [\mathbf{I}(\beta_0)]^{-1} \nabla l(\beta_0).$$

Using (3.2) in an iterative manner, we get the Newton–Raphson method for numerically determining the maximum likelihood estimate from any starting value β_0 . If the maximum likelihood estimate exists, the log-likelihood function is strictly concave, and we apply a suitable modification to the Newton–Raphson method (such as step-halving), then the method is guaranteed to converge to the maximum likelihood estimate from any starting value [see Kooperberg, Bose and Stone (1997) for details]. It follows from (3.1) and (3.2) that

$$(3.3) \quad 2[Q(\beta_1) - Q(\beta_0)] = [\nabla l(\beta_0)]^T [\mathbf{I}(\beta_0)]^{-1} \nabla l(\beta_0).$$

If β_0 is the maximum likelihood estimate in a subspace of \mathcal{B} , then the right-hand side of (3.3) is the Rao (score) statistic for testing the hypothesis that the “true” value of β lies in this subspace.

Let Q now be the quadratic approximation to the log-likelihood function about the maximum likelihood estimate $\hat{\beta} \in \mathcal{B}$, and let \mathcal{B}_0 be the subspace of \mathcal{B} consisting of all $\beta \in \mathcal{B}$ such that $\mathbf{A}\beta = \mathbf{0}$, where \mathbf{A} has full rank. Then the maximum of Q over \mathcal{B}_0 occurs uniquely at

$$(3.4) \quad \hat{\beta}_0 = \hat{\beta} - \mathbf{I}^{-1}(\hat{\beta}) \mathbf{A}^T [\mathbf{A} \mathbf{I}^{-1}(\hat{\beta}) \mathbf{A}^T]^{-1} \mathbf{A} \hat{\beta}.$$

Moreover,

$$(3.5) \quad 2[Q(\hat{\beta}) - Q(\hat{\beta}_0)] = (\mathbf{A} \hat{\beta})^T [\mathbf{A} \mathbf{I}^{-1}(\hat{\beta}) \mathbf{A}^T]^{-1} \mathbf{A} \hat{\beta}.$$

The right-hand side of (3.5) is the Wald statistic for testing the hypothesis that $\beta \in \mathcal{B}_0$ under the assumption that $\beta \in \mathcal{B}$. Moreover, the right-hand side of (3.4) gives a good starting value for using the Newton–Raphson method to find the maximum likelihood estimate in \mathcal{B}_0 when the maximum likelihood estimate $\hat{\beta}$ in \mathcal{B} has already been determined.

An important aspect of the methodology for fitting extended linear models is the adaptive choice of the space G from a family \mathcal{S} of allowable spaces that is typically assumed to satisfy the following properties:

1. For each $G \in \mathcal{S}$, the model has dimension $J \geq J_{\min}$.
2. There is only one $G \in \mathcal{S}$ with dimension J_{\min} , which we refer to as the minimum allowable space.
3. If $G_0 \in \mathcal{S}$ has dimension J , there is at least one space $G \in \mathcal{S}$ with dimension $J + 1$ that contains G_0 as a subspace.
4. If $G \in \mathcal{S}$ has dimension $J > J_{\min}$, there is at least one subspace $G_0 \in \mathcal{S}$ of G with dimension $J - 1$.

In our univariate methodologies (LOGSPLINE, LSPEC and HEFT) we use families of allowable spaces based on cubic splines. For each of these methodologies there are some extra restrictions on the allowable spaces, which are discussed in the relevant sections. Also, the HEFT and LSPEC methodologies involve some additional basis functions that are not cubic splines. Details are given in Sections 7 and 8.

For the multivariate methodologies POLYMARS (our version of MARS), POLYCLASS and HARE we make use of piecewise linear splines and selected tensor products. These spaces are discussed in detail in Section 5 about POLYMARS. In all of these applications we restrict attention to $d \leq 2$, so that main effects (polynomial splines in individual variables) and two-factor interactions (tensor products of polynomial splines in two different variables) may be allowed, but no three-factor or higher-order interactions are allowed in the model. The allowable spaces for the bivariate splines considered in Section 9 are discussed in that section.

Initially, we choose G as the minimum allowable space. Then we proceed with stepwise addition. Here we successively replace the $(J - 1)$ -dimensional allowable space G_0 by a J -dimensional allowable space G containing G_0 as a subspace, choosing among the various candidates for a new basis function by a heuristic search that is designed approximately to maximize the corresponding Rao statistic. The reason for using Rao statistics here is to avoid the need for computing maximum likelihood estimates corresponding to the various candidate spaces G .

Upon stopping the stepwise addition process (for example, after we reach a default or user-specified maximum dimension), we carry out stepwise deletion. Here we successively replace the J -dimensional allowable space G by a $(J - 1)$ -dimensional allowable subspace G_0 until we arrive at the minimal allowable space, at each step choosing the candidate space G_0 so that the Wald statistic for a basis function that is in G but not in G_0 is smallest in magnitude. The reason for using Wald statistics here is to avoid the need for

computing maximum likelihood estimates corresponding to the various candidate subspaces G_0 .

During the combination of stepwise addition and stepwise deletion, we get a sequence of models indexed by ν , with the ν th model having $J_\nu K$ parameters. The (generalized) Akaike information criterion (AIC) can be used to select one model from this sequence. Let \hat{l}_ν denote the fitted log-likelihood for the ν th model and let

$$(3.6) \quad \text{AIC}_{a,\nu} = -2\hat{l}_\nu + aJ_\nu K$$

be the Akaike information criterion with penalty parameter a for this model. We select the model corresponding to the value $\hat{\nu}$ of ν that minimizes $\text{AIC}_{a,\nu}$. In light of practical experience, we generally recommend choosing $a = \log n$ as in the Bayesian information criterion (BIC) due to Schwarz (1978). (Choosing $a = 2$ as in classical AIC tends to yield models that are unnecessarily complex, have spurious features and do not predict well on test data.)

Alternatively, we can use an independent test set to obtain a more nearly unbiased estimate of the expected log-likelihood and select the model that maximizes this estimate. In the regression and classification contexts we could use the independent test set to obtain a nearly unbiased estimate of the mean squared error of prediction or the cost of misclassification and select the model that minimizes this estimate.

Finally, cross-validation can be used to select a so as approximately to maximize the expected log-likelihood or minimize the expected mean squared error of prediction or cost of misclassification. [For detailed discussions of the use of independent test sets or cross-validation in the related context of selecting classification and regression trees, see Breiman, Friedman, Olshen and Stone (1984).]

Regardless of the final criteria used to choose between competing estimates, it is likely that many of the models encountered during the stepwise addition and deletion processes will perform similarly. By examining which terms are present in these best fitting models, we can gain considerable insight into the underlying features of the data. Simulation can also be used to judge whether or not our procedures can reliably resolve important aspects of a given data set. In addition, simulation can be used to calibrate the choice of (the implicit smoothing parameter) a in the AIC criterion of (3.6). Illustrations of these procedures will be given in the context of the various adaptive methodologies presented in Sections 4–9.

As mentioned in Section 1, various adaptive methodologies and corresponding software products have already been developed. The current situation regarding software availability is as follows:

1. Versions of the HARE, HEFT, LOGSPLINE and LSPEC methodologies are available from statlib. (The publicly available version of the LOGSPLINE program is slightly older than the one discussed in Section 4; see that section for more discussion.) All these methodologies are written as C programs with an interface to the S/S-PLUS environment.

2. A commercial version of HARE is currently being implemented in S-PLUS.
3. Friedman's MARS program is available as a collection of Fortran subroutines from statlib.
4. The POLYMARS program discussed in Section 5 was not written as a stand-alone program.
5. The current version of POLYCLASS is available from Kooperberg. We are working on a modification to this methodology to make it computationally much less intensive when applied to huge data sets with many classes, features and cases. In this modification we plan to use a stochastic gradient method to obtain the maximum likelihood fit to the largest model selected by POLYMARS.
6. A library of S/S-PLUS routines for manipulating Triogram models is currently available from Hansen and will soon be available in version 4 of S.

Our eventual goal is to develop a comprehensive set of polynomial spline modeling routines.

4. Univariate density estimation (LOGSPLINE). In logspline density estimation a (univariate) log-density is modeled by a cubic spline. The LOGSPLINE project was the first methodology project employing model selection and polynomial splines on which we have worked. In this section we describe the fourth version of LOGSPLINE. Earlier versions are discussed in Stone and Koo (1986b) and Kooperberg and Stone (1991, 1992). The various versions of LOGSPLINE all employ cubic splines and maximum likelihood estimation. The way that the program positions knots, how it deals with the tails of the distribution and what types of data it can handle are among the things that have evolved over time. Before presenting any details about the LOGSPLINE methodology, we give a brief example.

In the left side of Figure 1 we show a density estimate based on a random sample of 7125 annual net incomes in the United Kingdom [Family Expenditure Survey (1968–1983)]. [The data have been rescaled to have mean 1 as in Wand, Marron and Ruppert (1991).] The spike near 0.24 is due to the UK national old age pension, which caused many people to have nearly identical incomes. The right side of Figure 1 zooms in on the neighborhood of this spike. In Kooperberg and Stone (1992) we concluded that the height and location of this spike are accurately estimated by LOGSPLINE.

The selection of knots in logspline density estimation is discussed in detail below. Here it suffices to note that the procedure involves stepwise addition and deletion of knots. The program starts with a fairly small number of knots. In Figure 1 these knots are indicated by the letter "s". It then adds knots in those regions where an added knot would have the most influence, using Rao statistics. The program continues adding until a prespecified maximum number of knots is reached. The knots for this largest model are indicated by the letter "m" in Figure 1. After the largest model has been fitted, knots are deleted one at a time, using Wald statistics to decide which one to delete next. The smallest model that is fitted has three knots. Out of the complete

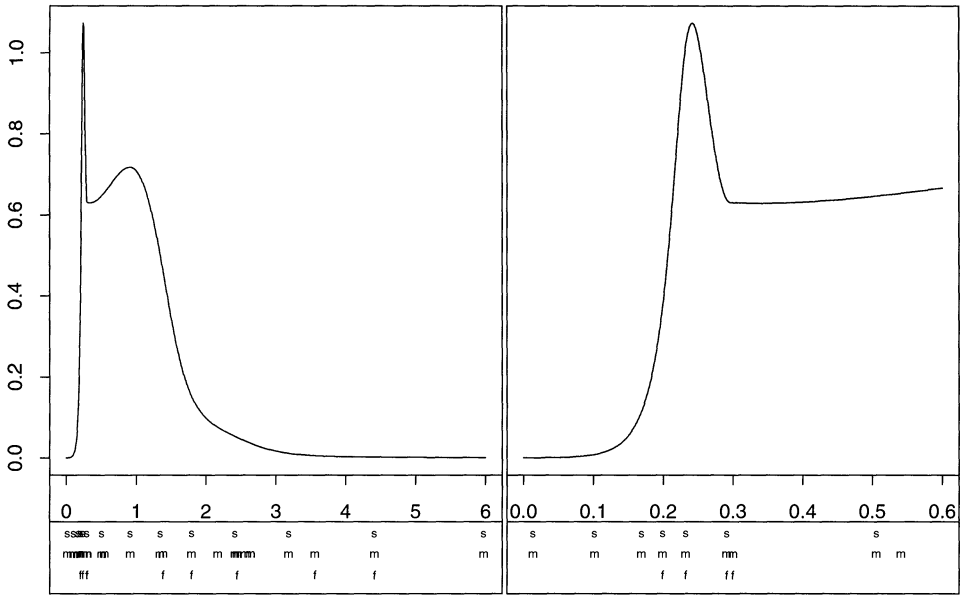


FIG. 1. Left: Log-spline density estimate for the income data. Right: Enlargement of the area near $x = 0.24$. The letters below the plots refer to the knot placement. See the text for details.

sequence of models, LOGSPLINE selects the one having the smallest value for the AIC criterion. The knots for this “best” model are indicated by the letter “f” in Figure 1.

Usually, as is the case here, the final model based on the AIC criterion is fitted during the stepwise deletion stage of the procedure. The new LOGSPLINE procedure thus has the advantage that it adds knots in those parts of the density where they are most needed, for example, near the spike, while it deletes knots where they are not needed, for example, in the tails, thus creating an adaptivity that other density estimation procedures seem to lack. This is one of LOGSPLINE’s main advantages.

LOGSPLINE has additional advantages over other density estimation methods:

1. While LOGSPLINE generally gives accurate estimates of the height and location of peaks, thanks to adaptivity, it avoids spurious bumps and gives smooth estimates in the tail of the distribution.
2. LOGSPLINE has a natural way to estimate densities with bounded support, which may be discontinuous at the end of their range.
3. LOGSPLINE can estimate the density even when some observations are censored.
4. A LOGSPLINE density is represented by a list of numbers of moderate length, making it convenient to use the density for further analysis.

The LOGSPLINE method is fairly fast: on our Sparc 10 workstation the estimate shown in Figure 1 was computed in about 9 s of CPU time.

In the following section we will discuss the LOGSPLINE methodology in some detail. In Section 4.2 we present an example of the application of the various LOGSPLINE algorithms to a much smaller data set.

4.1. *The LOGSPLINE methodology.*

LOGSPLINE models. As usual in our polynomial spline methodologies, there are two main issues to LOGSPLINE:

1. Given a linear space, how are the parameters estimated?
2. How is the linear space selected?

We now discuss the types of linear spaces that we consider in LOGSPLINE and the corresponding log-likelihood function. Then we discuss how to select a linear space in an adaptive manner.

Given the integer $K \geq 3$, the numbers L and U with $-\infty \leq L < U \leq \infty$ and the sequence t_1, \dots, t_K with $L < t_1 < \dots < t_K < U$, let G be the space of twice continuously differentiable functions s on (L, U) such that the restrictions of s to $[t_1, t_2], \dots, [t_{K-1}, t_K]$ are cubic polynomials and the restrictions of s to $(L, t_1]$ and $[t_K, U)$ are linear. The space G is K -dimensional. Set $J = K - 1$. Then G has a basis of the form $1, B_1, \dots, B_J$. We can choose B_1, \dots, B_J such that B_1 is linear with negative slope on $(L, t_1]$, B_2, \dots, B_J are constant on $(L, t_1]$, B_J is linear with positive slope on $[t_K, U)$ and B_1, \dots, B_{J-1} are constant on $[t_K, U)$.

A column vector $\beta = (\beta_1, \dots, \beta_J)^T \in \mathbb{R}^J$ is said to be *feasible* if

$$\int_L^U \exp(\beta_1 B_1(y) + \dots + \beta_J B_J(y)) dy < \infty$$

or, equivalently, if (i) either $L > -\infty$ or $\beta_1 < 0$ and (ii) either $U < \infty$ or $\beta_J < 0$. Let \mathcal{B} denote the collection of such feasible column vectors. Given $\beta \in \mathcal{B}$, set

$$f(y; \beta) = \exp(\beta_1 B_1(y) + \dots + \beta_J B_J(y) - C(\beta)), \quad L < y < U,$$

where

$$C(\beta) = \log \left(\int_L^U \exp(\beta_1 B_1(y) + \dots + \beta_J B_J(y)) dy \right).$$

Then $f(\cdot; \beta)$ is a positive density function on (L, U) for $\beta \in \mathcal{B}$. If $U = \infty$, then the density function is exponential on $[t_K, \infty)$; if $L = -\infty$, then the density function is exponential on $(-\infty, t_1]$.

Let Y_1, \dots, Y_n be a random sample of size n from a distribution on (L, U) having density function f . Let A_1, \dots, A_n be subintervals of (L, U) such that it is known only that $Y_i \in A_i$ for $1 \leq i \leq n$. If Y_i is uncensored, then $A_i = \{Y_i\}$. If Y_i is right censored at $C_i < Y_i$, then $A_i = (C_i, U)$. If Y_i is left censored at $C_i > Y_i$, then $A_i = (L, C_i)$. In either case, we refer to C_i as the censoring value of Y_i . If Y_i is interval censored, then its censoring interval A_i is a subinterval of (L, U) . Under the usual assumption that the random

sample is independent of the censoring mechanism, the log-likelihood function corresponding to the LOGSPLINE model has the form given by

$$l(\boldsymbol{\beta}) = \sum_i \varphi(A_i; \boldsymbol{\beta}), \quad \boldsymbol{\beta} \in \mathcal{B};$$

here

$$\varphi(y; \boldsymbol{\beta}) = \log f(y; \boldsymbol{\beta}) = \sum_j \beta_j B_j(y) - C(\boldsymbol{\beta}), \quad \boldsymbol{\beta} \in \mathcal{B},$$

if A is the one-point set $\{y\}$ and

$$\varphi(A; \boldsymbol{\beta}) = \log \left(\int_A f(y; \boldsymbol{\beta}) dy \right) = \log \left(\int_A \exp \varphi(y; \boldsymbol{\beta}) dy \right), \quad \boldsymbol{\beta} \in \mathcal{B},$$

if A has positive length. Formulas for the score function and Hessian can be found in Kooperberg and Stone [(1992), Section 2]. These formulas become rather complicated when A has positive length.

The maximum likelihood estimate $\hat{\boldsymbol{\beta}}$ is given by $l(\hat{\boldsymbol{\beta}}) = \max_{\boldsymbol{\beta} \in \mathcal{B}} l(\boldsymbol{\beta})$, and the log-likelihood of the fitted model is given by $\hat{l} = l(\hat{\boldsymbol{\beta}})$. The corresponding maximum likelihood estimate of f is given by $\hat{f}(y) = f(y; \hat{\boldsymbol{\beta}})$ for $L < y < U$.

Model selection. The knot selection methodology involves initial knot placement, stepwise knot addition, stepwise knot deletion and final model selection based on AIC. In this subsection we assume that all the data are uncensored; that is, $A_i = \{Y_i\}$ for all i .

Initially we start with K knots, with $K = \min(2.5n^{1/5}, n/4, N, 25)$, where N is the number of distinct Y_i 's. These K knots are positioned according to the rule described in Kooperberg and Stone (1992). This rule places knots at selected order statistics of the data. (The rule is suitably modified when some data are censored.) If $L = -\infty$ and $U = \infty$, the extreme knots are placed at the extreme observations and the interior knots are positioned such that the distances (on an order statistic scale) between knots near the extremes of the data are fairly small and almost independent of the sample size, while the knots in the interior are positioned approximately equidistantly. If $L > -\infty$ or $U < \infty$, the procedure is suitably modified.

The knot-addition/knot-deletion procedure that we employ is essentially the procedure described in Section 3. In particular, at each addition step of the algorithm we first find a good location for a new knot in each of the intervals (L, t_1) , (t_1, t_2) , \dots , (t_{K-1}, t_K) , (t_K, U) determined by the existing knots t_1, \dots, t_K . To do this we maximize in each interval the Rao statistic for potential knots located at the quartiles of the data within each interval. The location is then further optimized, which may involve computing a few more Rao statistics [see Section 11.3 of Kooperberg, Stone and Truong (1995a) for our current implementation]. The search algorithm then selects among the best candidates within the various intervals. The default value for the maximum number of knots in a model is $K_{\max} = \min(4n^{1/5}, n/4, N, 30)$.

During knot deletion we successively remove the least significant knot, where Wald statistics are used to measure significance. We continue this procedure until only three knots are left. (Rarely, with extremely heavy tailed densities, there are numerical problems when the number of knots is too small. In such a situation we terminate the procedure as soon as these problems occur.)

Among all models that are fitted during the sequence of knot addition and knot deletion we choose the model that minimizes AIC with default penalty parameter $a = \log n$, as described in Section 3.

Innovations. As we mentioned in the introduction to this section, the present version of LOGPSLINE is the fourth version. In the first version [Stone and Koo (1986b)], a small fixed number of knots was placed equidistantly on an order-statistic logit scale. In Kooperberg and Stone (1991), stepwise knot deletion was employed, and the initial knot placement rule was very similar to the one we now employ. Both of these earlier papers used a preliminary transformation for densities on the positive half-line. In Kooperberg and Stone (1992) it was decided that such a transformation is not needed when the knot placement is sufficiently adaptive. In the 1992 paper we extended logspline density estimation to censored data and discussed a user interface based on S. The present version of LOGSPLINE is the only one that includes stepwise addition of knots. There are also several significant computational improvements, the two most important of which are as follows:

1. The starting values used during stepwise deletion are obtained by maximizing a quadratic approximation to the log-likelihood function, as described in Section 3. These starting values are significantly better than those proposed in Kooperberg and Stone (1992). Indeed, the number of Newton–Raphson iterations may be reduced by as much as 30%.
2. In the absence of censored data the log-likelihood function is strictly concave. Therefore, if a maximum of the log-likelihood function exists, it is unique. If some of the observations are censored, however, the log-likelihood function need not be concave. In Kooperberg and Stone (1992), this problem was circumvented by alternating between Newton–Raphson and steepest ascent. We now take the approach of adding a small negative constant times the identity matrix to the Hessian, if necessary, to ensure that this matrix is negative definite [see Kennedy and Gentle (1980), Section 10.2.2].

Note that the version of the program described in Kooperberg and Stone (1992) is available from statlib (statlib@stat.cmu.edu). The version described in this paper is not yet publicly available.

4.2. An example. The penalty parameter a in the AIC criterion (see Section 3) is the main parameter in the LOGSPLINE procedure that governs the complexity of the final density estimate. The default value for this parameter is $a = \log n$ as in BIC. Another commonly used value is $a = 2$ as in (traditional) AIC. One of the goals of this section is to study the influence of this penalty parameter by means of a small simulation study.

Besides the choice of the penalty parameter, it may matter whether we use the new LOGSPLINE procedure, as described in this paper, or the previous LOGSPLINE procedure, described in Kooperberg and Stone (1992). Since the new procedure positions some of the knots adaptively, so as approximately to maximize the log-likelihood, conceivably it may lead to a more flexible estimate.

We applied the new and previous LOGSPLINE procedures with both $a = 2$ and $a = \log n$ to the Buffalo snowfall data. This is a small data set ($n = 63$) that has been used extensively in the density estimation literature; see, for example, Parzen (1979) and Silverman (1986). The main issue here is the number of modes: is there one or are there three (or maybe two)? As can be seen from Figure 2, the different LOGSPLINE procedures provide different answers, as summarized in Table 1. From this table we see that the model that was selected using the new procedure with penalty parameter $a = 2$ would also have been selected for values of a between 0.45 and 3.01. From (3.6) we note that if a model with J basis functions is selected for some value of a , it will be selected for a range of values of a . Some models may not be

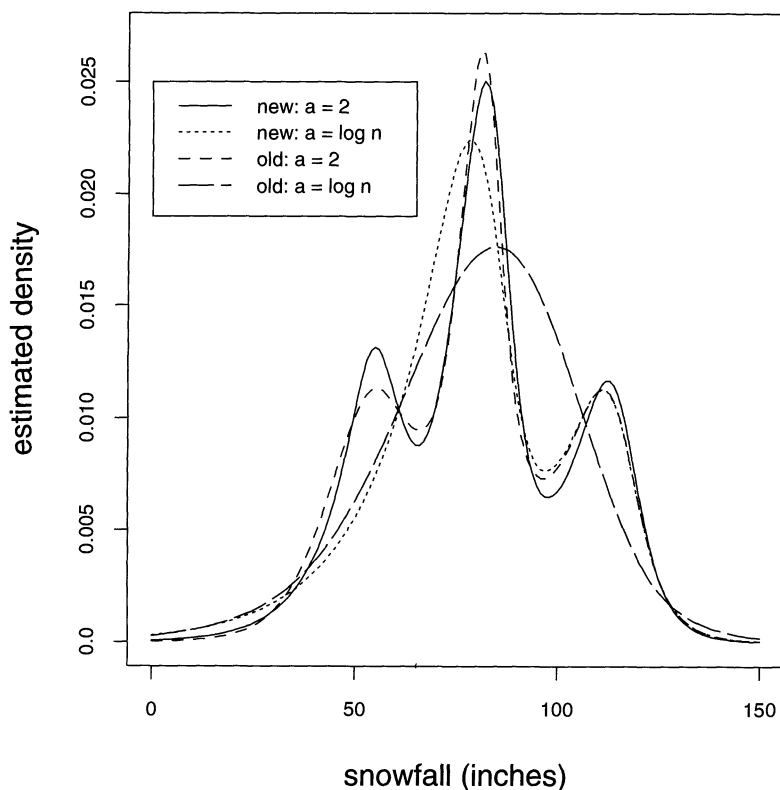


FIG. 2. Log spline density estimates for the Buffalo snowfall data ($n = 63$) for the new and the previous LOGSPLINE procedure and two different values of the penalty parameter.

TABLE 1
Knots and modes for LOGSPLINE estimates for the Buffalo snowfall data

Procedure	Optimal for a		Number of Knots	Number of Modes
	From	To		
New procedure, $a = 2$	0.45	3.01	7	3
New procedure, $a = \log n \approx 4.14$	3.01	8.38	5	2
Previous procedure, $a = 2$	0.03	2.65	7	3
Previous procedure, $a = \log n \approx 4.14$	2.65	∞	3	1

optimal for any value of a [see Kooperberg, Stone and Truong (1995a), Table 6]. Note that for $n = 63$ the starting number of knots for the previous procedure is 10, while for the new procedure it is 6, with 4 knots being added by the algorithm.

To investigate the behavior of the LOGSPLINE estimation procedures in situations similar to the snowfall data, we generated 100 samples of size 63 from each of the densities shown in Figure 2, except for the estimate of the previous procedure with $a = 2$ since it is very similar to the estimate of the new procedure with $a = 2$. For each of the 300 samples that we obtained, we applied the same procedures with the same choices of a as in Figure 2, yielding four estimates for each sample. In Table 2 we summarize the number of modes in each of these estimates. Not unexpectedly, the procedures with $a = \log n$ tend to underestimate the number of modes, while the procedures with $a = 2$ tend to overestimate it. Although it would be possible to fine tune the penalty parameter to balance the number of times the procedure underestimates and overestimates the number of modes, we feel that it may be more useful to look at a few estimates with different values of the penalty parameter before deciding on the final estimate. From Table 2 we also see that the newer procedures are indeed a little more flexible than the old procedures, yielding even more overestimation of the number of modes for the $a = 2$ procedure, while the new procedure with $a = \log n$ falls in between the two old procedures. From this summary we thus see that with the present sample size it is virtually impossible to distinguish accurately between densities with one, two and three modes. However, when we generated samples from the

TABLE 2
Number of modes in the simulation study with $n = 63^$*

Data generated from:	Previous $a = \log n$				New $a = \log n$				New $a = 2$			
Correct number of modes:	1				2				3			
Estimated number of modes:	1	2	3	≥ 4	1	2	3	≥ 4	1	2	3	≥ 4
New $a = 2$	39	41	19	1	7	74	17	2	6	26	64	4
New $a = \log n$	74	23	3	0	34	64	2	0	29	40	31	0
Previous $a = 2$	51	37	11	1	16	68	16	0	12	22	65	1
Previous $a = \log n$	84	13	3	0	51	46	3	0	45	26	29	0

*The numbers of estimates having the correct number of modes are boldface.

TABLE 3
Number of modes in the simulation study with $n = 250^$*

Data generated from:	Previous $a = \log n$				New $a = \log n$				New $a = 2$			
	Correct number of modes:											
	1	2	3	≥ 4	1	2	3	≥ 4	1	2	3	≥ 4
New $a = 2$	41	26	25	8	0	56	32	12	0	3	68	29
New $a = \log n$	88	12	0	0	4	90	4	2	0	9	89	2
Previous $a = 2$	74	19	7	0	2	79	18	4	0	9	90	1
Previous $a = \log n$	99	1	0	0	16	82	2	0	5	17	78	0

*The numbers of estimates having the correct number of modes are boldface.

unimodal density (previous procedure, $a = \log n$) and estimated the density with one of the procedures with $a = 2$, we noticed that when we got two modes, the second mode was more often on the left side of the main mode than on the right side. This is not surprising since the density is slightly flatter on that side. Reversing this reasoning we are lead to believe that the existence of a side mode to the right of the main mode is more plausible than the existence of a side mode to the left of the main mode.

Although all procedures have trouble distinguishing between unimodal and multimodal densities when $n = 63$, most carry out this task well when the sample size gets larger. In Table 3 we summarize a similar simulation study as in Table 2, except that we generated samples of size 250 from the densities in Figure 2. For this sample size the starting number of knots for the previous procedure is 12, while the new procedure starts with eight knots and adds four more during the algorithm. Except for the new procedure with $a = 2$, all methods get the right number of modes at least 74% of the time. The new method with $a = \log n \approx 5.52$ gets it right at least 88% of the time for each of the three situations.

5. Regression (MARS). When viewing regression as a function estimation problem we recognize that the regression function may not be a linear additive function of the predictors and instead allow nonlinear and possibly also nonadditive functions. When there is only one predictor, nonparametric regression can be viewed as smoothing, for which there are numerous methods available. Some of the popular methods are kernel and local polynomial regression [Wand and Jones (1995); Fan and Gijbels (1996)], smoothing splines [Wahba (1990); Green and Silverman (1994)], and polynomial splines. Smith (1982) wrote the first paper to use polynomial splines with adaptively selected knots for regression problems. In her method, knots for cubic splines are positioned uniformly over the range of the data, after which a stepwise knot deletion algorithm is employed.

While many of the univariate nonparametric regression methods can be generalized to situations where there are a few predictors, the curse of dimensionality applies when there are many predictors. One attractive approach for ameliorating this curse is to model the regression function as an additive

function of the predictors. This approach has been popularized by Hastie and Tibshirani (1990), who treat both linear regression and generalized regression, including logistic regression and Poisson regression, and emphasize the use of backfitting together with a one-dimensional smoother to fit additive models to data.

An early paper using polynomial splines for additive linear regression as well as additive logistic regression is Stone and Koo (1986a), in which knots were placed at nonadaptive (predetermined) quantiles. Stepwise knot selection, forward and backward, was used in the additive regression program TURBO by Friedman and Silverman (1989). A somewhat different approach to additive regression involving stepwise knot selection was developed by Breiman (1993). In the applications of cubic splines in these papers, linear constraints were placed on the tails of the splines mainly to control the variance of the corresponding estimates.

When nonadditive models are considered, the usual approach to nonparametric regression has been to restrict the model to additive main effects and selected low-order interactions. Gu and Wahba (1993) developed a smoothing spline approach to ANOVA modeling in function estimation. Friedman (1991) introduced multivariate adaptive regression splines (MARS), which is a polynomial spline methodology for estimating the regression function.

In this section we first give a brief description of Friedman's MARS program. When we were working on POLYCLASS [Kooperberg, Bose and Stone (1997)], we found it necessary to develop our own version of MARS to handle very large data sets with many predictors and basis functions. In Section 5.2 we describe this version of MARS and list some differences between our version and Friedman's version. In Section 5.3 we present a small example in which we compare the two programs.

From now on, when we mention "MARS" in this paper, we refer either to Friedman's version or to both versions simultaneously. We refer to our version of the MARS algorithm as "POLYMARS."

5.1. *MARS.* Let $(\mathbf{X}_1, Y_1), \dots, (\mathbf{X}_n, Y_n)$ denote a random sample from the distribution of (\mathbf{X}, Y) , where $\mathbf{X} \in \mathbb{R}^M$ and $Y \in \mathbb{R}$. We wish to estimate $f(\mathbf{X}) = E(Y|\mathbf{X})$. The MARS model [Friedman (1991)] can be written as

$$(5.1) \quad f(\mathbf{X}) = f(\mathbf{X}|\boldsymbol{\beta}) = \sum_{j=1}^J \beta_j B_j(\mathbf{X}).$$

For a given set of basis functions, the unknown parameters in MARS are estimated using least squares. The selection of the basis functions in MARS is not easily written in the allowable spaces framework of Section 3. Here we outline the main features of the MARS algorithm when piecewise linear splines are used. A refinement of this algorithm makes use of continuously differentiable functions that are similar, but not exactly identical to the cubic splines employed in various other sections of this paper. (Note that these cubic splines yield twice continuously differentiable functions.)

In the MARS program the one-dimensional model $f(\mathbf{x}) = \beta_1$ is initially fitted. Then, successively, models with J basis functions are replaced by models with $J + 1$ or $J + 2$ basis functions. This is done by considering the addition of all possible pairs of new basis functions $B_m(\mathbf{x})(x_i - t)_+$ and $B_m(\mathbf{x})(t - x_i)_+$, where x_i is one of the predictors, t is a new knot in that predictor and $B_m(\mathbf{x})$ is a basis function currently in the model that does not depend on x_i . [Some of these additions may involve adding only one genuinely new basis function since one new basis function would already be in the span of the existing basis functions and the other new basis function; see Friedman (1991).] In the MARS algorithm every data coordinate that is sufficiently far from existing knots for the corresponding variable is a candidate for a new knot for that variable. The best model of dimension $J + 2$ or $J + 1$ is chosen among such candidates for stepwise addition using a generalized cross-validation (GCV) criterion. The stepwise addition of basis functions continues until a user-specified maximum number of basis functions is reached. During the stepwise deletion stage of MARS, any of the nonconstant basis functions can be removed at any step. GCV is used to select the best overall model during the addition or deletion stage.

An option in MARS allows the user to restrict each basis function to depend on at most d predictors. The POLYMARS methodology described below corresponds to MARS with $d = 2$.

5.2. POLYMARS. The setup for POLYMARS is identical to that for MARS, except that with POLYCLASS (Section 6) in mind we allow the response Y to be in \mathbb{R}^K with $K \geq 1$. For simplicity, however, we will assume here that $K = 1$ since all computations generalize trivially. As in the other methodologies, we model $f(\mathbf{X})$ in a linear space, so that (5.1) again holds.

For POLYMARS it is convenient to define an allowable space by listing its basis functions. For $1 \leq m \leq M$, let J_m be an integer with $J_m \geq -1$; if $J_m = -1$ there are no basis functions depending on x_m ; if $J_m = 0$, consider the basis function $B_{m0}(x_m) = x_m$; if $J_m \geq 1$, consider the basis function $B_{m0}(x_m) = x_m$, let x_{mj} for $1 \leq j \leq J_m$ be distinct real numbers, and consider the additional basis functions $B_{mj}(x_m) = (x_m - x_{mj})_+$ for $1 \leq j \leq J_m$.

Let G be the linear space having basis functions $1, B_{mj}(x_m)$ for $1 \leq m \leq M$ and $0 \leq j \leq J_m$, and perhaps certain tensor products of two such basis functions. It is required that if $B_{lj}(x_l)B_{mk}(x_m)$ be among the basis functions for some $j \geq 1$, then $B_{l0}(x_l)B_{mk}(x_m) = x_l B_{mk}(x_m)$ and hence (if $k > 0$) $x_l x_m$ be among the basis functions.

One reason for adding linear terms before knots and main effects before interactions is to yield models that are simpler and easier to interpret. A second reason is to reduce the variance associated with the overall modeling procedure, and a third is to reduce the likelihood of ending up with spurious terms in the final model. The requirement of adding main effects before interactions is also motivated by theoretical considerations regarding convergence rates (see Section 2).

It is easy to check that the collection \mathcal{S} of such spaces satisfies the properties listed in Section 3. In particular, the minimal allowable space G_{\min} for the POLYMARS model is the space of constant functions. Thus the minimal model for (5.1) has $J = 1$, $B_1 = 1$ and $f(\mathbf{X}) = \beta_1$ so that $f(\mathbf{X})$ does not depend on the vector \mathbf{X} of predictors. Note that the highest order d of interactions allowed in a POLYMARS model is two.

Given the basis of an allowable space G as defined above, it is obvious whether any given basis function can be deleted in one step.

EXAMPLE. Let $M = 4$, $B_1 = 1$, $B_2 = x_1$, $B_3 = (x_1 - 1)_+$, $B_4 = x_2$, $B_5 = x_3$ and $B_6 = x_1x_2$. Then B_1, \dots, B_6 span an allowable space G . In this example, B_3 , B_5 or B_6 could be removed and the remaining space would still be allowable. If one of the basis functions B_2 or B_4 were removed, however, the remaining space would not be allowable since it would still contain $B_6 = B_2B_4$ (as well as B_3 in the case of removing B_2). The constant basis function B_1 can never be removed.

Let G_0 be the allowable space having basis functions $1, B_{mj}(x_m)$ for $1 \leq m \leq M$ and $1 \leq j \leq J_m$, and perhaps certain tensor products of two such basis functions. To decide which basis function to add to this model, we compute the Rao statistic as described in Section 3:

(i) For all spaces that can be obtained from G_0 by adding a basis function $B_{l0}(x_l) = x_l$ to G_0 ;

(ii) for all allowable spaces that can be obtained from G_0 by adding a basis function to G_0 that is a tensor product of two basis functions $B_{lj}(x_l)$ and $B_{mk}(x_m)$, $l \neq m$, that are in G_0 ;

(iii) for an allowable space that can be obtained from G_0 by adding a basis function corresponding to a potential new knot in predictor m for $1 \leq m \leq M$. For every predictor we consider a fixed number N_0 of potential new knots, which typically are preselected order statistics of the data.

As the new space G we choose the one corresponding to the largest absolute value of the Rao statistic among those candidates listed above that are nonvacuous.

EXAMPLE (Continued). Corresponding to (i), we can add the basis function x_4 to the space in the above example. Corresponding to (ii), we can add $B_2B_5 = x_1x_3$, $B_3B_4 = (x_1 - 1)_+x_2$ or $B_4B_5 = x_2x_3$ to the space. The basis function $B_3B_5 = (x_1 - 1)_+x_3$ cannot be added, since the resulting space would not contain $B_2B_5 = x_1x_3$ so it would not be allowable. Corresponding to (iii), a basis function $(x_1 - x_{1k})_+$ with $x_{1k} \neq 1$, $(x_2 - x_{2k})_+$ or $(x_3 - x_{3k})_+$ could be added. No basis function of the form $(x_4 - x_{4k})_+$ could be added before x_4 is added.

For a given allowable space, the parameters β_j in (5.1) can be estimated using least squares. The Rao and Wald statistics that are used to decide which

basis function to add or delete now reduce to the difference in the residual sum of squares between two nested models. The AIC criterion to select the final model is replaced by a penalized residual sum of squares called GCV [Friedman, (1991)]. In particular, we select the model that minimizes

$$\frac{\text{RSS}_J}{n} \bigg/ \left[1 - \frac{a(J-1)}{n} \right]^2,$$

where RSS_J is the residual sum of squares for the model with J basis functions and a is a parameter that we typically set equal to 2.5.

Several computational tricks make it possible for the POLYMARS algorithm to be extremely fast, even for huge data sets and many basis functions. [See Kooperberg, Bose and Stone (1997) for more details.] In particular, since we limit the number of potential locations for new knots, inner products need to be computed at most once. If the maximum number of basis functions considered is P_{\max} , the complete POLYMARS program requires $O(N_0 n P_{\max}^2)$ floating point operations (flops), while MARS (which has to recompute inner products since there are too many candidate basis functions to store them all) requires $O(M n P_{\max}^3)$ flops. In particular, on an example with $n = 10,000$, $M = 63$, $N_0 = 20$ and $P_{\max} = 80$, the POLYMARS program required 474 s of CPU time, while MARS required 12,636 s on the same machine.

Besides these computational issues, there are other differences between MARS and POLYMARS:

1. The allowable spaces are different. This is most evident in the addition stage, during which we add first a linear term and perhaps later a knot, while in Friedman's program two basis functions, essentially corresponding to a linear function and a knot, are added at the same time.
2. During the deletion stage POLYMARS requires interaction basis functions to be removed before the corresponding main effects can be removed. Knots have to be removed before linear terms are removed. MARS has no such restrictions.
3. In MARS, but not in POLYMARS, a piecewise cubic approximation to the piecewise linear function is applied after a basis function is added.

5.3. An example. For a comparison of the two MARS programs on a small data set, we applied them to the well studied Boston housing data [see, e.g., Belsley, Kuh and Welsch (1980) and Breiman, Friedman, Olshen and Stone (1984)]. The response is the median value of homes in thousands of dollars and there are 13 predictors, many of which are highly collinear.

In our experiment we randomly divided the data into a training set of 304 cases and a test set of 202 cases. Both MARS programs were applied to the training set, using 30 as the maximum number of basis functions, GCV to select the final model and otherwise the default options in both programs. (In MARS we set the maximum number of terms in each basis function equal to 2, to make the program comparable to POLYMARS.) We then computed the mean squared error (MSE) on the test set. We repeated this experiment 10

TABLE 4
MARS fits for the Boston housing data

Method	MSE	CPU
MARS, linear fit	14.37	5.07
MARS, cubic approximation	15.91	5.07
POLYMARS	14.07	3.41

times. The results are summarized in Table 4, together with the average cpu time on our SGI workstation. Since MARS supplies both a piecewise linear fit and a piecewise cubic approximation to this fit, there are two MSE's for this program. The standard errors in the estimates of the mean squared error are all approximately 1.5, while the variation in the CPU times is negligible. Over these 10 repetitions, the correlation between the MSE of the POLYMARS fit and that of the piecewise linear MARS fit is 0.94, while the two other correlations are between 0.4 and 0.6. From this table we see that the difference between the two piecewise linear fits is negligible, while both are a little better than the piecewise cubic approximation.

We then applied both MARS procedures to the complete data, with 80 as the maximum number of basis functions. MARS used 78.6 s CPU time to select 53 basis functions, while POLYMARS used 33.7 s to select 41 basis functions. Both models were very complicated: for example, POLYMARS used 10 of the 13 covariates, and 12 pairs of covariates had at least one tensor-product basis function involving both covariates in the pair. MARS used 11 of the 13 covariates, and 22 pairs of covariates had at least one tensor-product basis function involving both covariates in the pair.

6. Polychotomous regression and multiple classification (POLYCLASS).

6.1. *The POLYCLASS model.* The multiple classification problem is well studied in statistics. Typically, there is a qualitative random variable Y that takes on a finite number $K + 1$ of values, which we refer to as classes. Based on a vector of predictors $\mathbf{X} \in \mathbb{R}^M$, we want to predict Y .

In POLYCLASS we use piecewise linear splines and selected tensor products ($d \leq 2$) to model the conditional class probabilities. Specifically, suppose $P(Y = k | \mathbf{X} = \mathbf{x}) > 0$ for $k \in \mathcal{K} = \{1, \dots, K + 1\}$ and $\mathbf{x} \in \mathcal{X}$, where \mathcal{X} is a subset of \mathbb{R}^M over which \mathbf{X} ranges. Set

$$\theta(k|\mathbf{x}) = \log \frac{P(Y = k | \mathbf{X} = \mathbf{x})}{P(Y = K + 1 | \mathbf{X} = \mathbf{x})}, \quad \mathbf{x} \in \mathcal{X} \text{ and } k \in \mathcal{K}.$$

Then $\theta(K + 1|\mathbf{x}) = 0$ for $\mathbf{x} \in \mathcal{X}$ and

$$(6.1) \quad P(Y = k | \mathbf{X} = \mathbf{x}) = \frac{\exp \theta(k|\mathbf{x})}{\exp \theta(1|\mathbf{x}) + \dots + \exp \theta(K + 1|\mathbf{x})},$$

$\mathbf{x} \in \mathcal{X}$ and $k \in \mathcal{K}$.

We refer to (6.1) as the *polychotomous regression model*; when $K = 1$ it is referred to as the *logistic regression model*.

Let J be a positive integer and let G be a J -dimensional linear space of functions on \mathcal{X} with basis B_1, \dots, B_J . Consider the model

$$(6.2) \quad \theta(k|\mathbf{x}) = \theta(k|\mathbf{x}; \boldsymbol{\beta}_k) = \sum_{j=1}^J \beta_{jk} B_j(\mathbf{x}), \quad \mathbf{x} \in \mathcal{X} \text{ and } k \in \mathcal{K};$$

here $\boldsymbol{\beta}_k = (\beta_{k1}, \dots, \beta_{kJ})^T$ for $1 \leq k \leq K$, $\boldsymbol{\beta}_{K+1} = 0$ and $\boldsymbol{\beta}$ is the JK -dimensional column vector consisting of the entries of $\boldsymbol{\beta}_1, \dots, \boldsymbol{\beta}_K$, which range over $\mathcal{B} = \mathbb{R}^{JK}$. Correspondingly, set

$$P(Y = k|\mathbf{X} = \mathbf{x}; \boldsymbol{\beta}) = \frac{\exp \theta(k|\mathbf{x}; \boldsymbol{\beta})}{\exp \theta(1|\mathbf{x}; \boldsymbol{\beta}) + \dots + \exp \theta(K+1|\mathbf{x}; \boldsymbol{\beta})}$$

for $\boldsymbol{\beta} \in \mathcal{B}$, $\mathbf{x} \in \mathcal{X}$ and $k \in \mathcal{K}$.

In POLYCLASS the basis functions $B_j(\mathbf{x})$ that are used in (6.2) are piecewise linear splines and their selected tensor products. Based on sample data, the coefficients β_{jk} can be estimated by maximum likelihood, yielding a concave optimization problem; see Kooperberg, Bose and Stone (1997) for more details.

As in most of the procedures that we describe in this paper, we use stepwise addition based on Rao statistics and stepwise deletion based on Wald statistics to select the basis functions. Some details specific to POLYCLASS are discussed in Section 6.3. The model selection in POLYCLASS can be carried out using AIC, an independent test set or cross-validation [see Kooperberg, Bose and Stone (1997)].

6.2. A phoneme recognition example. In Kooperberg, Bose and Stone (1997), POLYCLASS is applied to a huge data set from the area of speech recognition. Here we present an abbreviated version of this analysis. The source of this data set is the Center for Spoken Language Understanding in Portland, Oregon [Cole, Roginski and Fanty (1992); Cole et al. (1994)]. It consists of 2165 utterances from telephone calls, which are numbers that typically are parts of addresses, zip codes and street numbers. Each utterance was processed by one or more listeners, who produced a time-aligned phonetic description of the utterance. For example, for one particular utterance, "3o3" (three-oh-three), it was determined that from 1 to 167 ms, the speaker produced phoneme T, followed by phoneme r from 167 to 193 ms and so on. It should be noted that the person who decided which phoneme was spoken was not aware of the text of the utterance. The phoneme transcription, which we obtained from the International Computer Science Institute (ICSI) in Berkeley, California, is based on the LIMSI phonetic alphabet [Gauvain, Lamel, Adda and Adda-Decker (1994)].

The utterances were also processed to produce perceptual linear predictive (PLP) features. Every 12.5 ms the audible spectrum, based on a concen-

tric 25 ms piece of sound, is determined. Since we consider telephone data, which is sampled at the frequency of 8 kHz, there are 200 observations of the sound wave in such a 25 ms interval. A Hamming window is applied to these 200 observations before the spectrum is estimated using the discrete Fourier transform. The estimated spectrum is next transformed to yield a critical-band integrated power spectrum with an equal-loudness preemphasis and a cube root nonlinearity to simulate the auditory intensity–loudness relation. Then the eighth-order autoregressive all-pole model of the transformed spectrum is obtained. The coefficients of the Fourier transform representation of the log-magnitude of this model are known as its cepstral coefficients. The PLP features [Boulevard and Morgan (1994); Hermansky (1990); Rabiner and Juang (1993)] that we used are the log-gain of the model (similar to the variance) and the next eight cepstral coefficients (similar to the autoregressive coefficients).

The goal in our analysis is to estimate the probability distribution over all phonemes at intervals of 12.5 ms based on the (nine) features available at that time point as well as the features available at the c time points, each 12.5 ms apart, before and after the point at which we want to estimate the phoneme distribution.

Such a probability distribution (or, more precisely, a likelihood that is obtained by weighting the estimated probabilities by the empirically determined frequencies of the phonemes) can be used as input to train (estimate) a hidden Markov model, which in turn can be used for automatic speech recognition [Boulevard and Morgan (1994)]. In the hybrid approach described by Boulevard and Morgan, a multilayer perceptron network (a type of artificial neural network) is used to estimate these probabilities.

There were 45 different phonemes, yielding 247,039 cases (12.5 ms intervals). We randomly divided the data into a training set of approximately 112,000 cases and a test set of about 135,000 cases. We used the vector of features at seven different time points, so that $c = 3$ above. The eight cepstral coefficients were used exactly as we received them from ICSI. Since some speakers speak more loudly than others, the log-gain by itself is not an informative predictor of the phoneme that is being spoken. Differences in the log-gain may be more informative. If $e(i)$ is the log-gain at time instance i , we used

$$d(i) = e(i) - \frac{1}{7} \sum_{j=-3}^3 e(i+j)$$

instead of $e(i)$.

The standard POLYCLASS methodology would be practically impossible to apply to the phoneme recognition data, for which $K = 44$, $M = 9 \cdot 7 = 63$ and the sample size is given by $n = 112, 115$. In Kooperberg, Bose and Stone (1997) a number of modifications, which make it possible for POLYCLASS to deal with this data set, are discussed. The most important such modification is that instead of computing the regular Rao statistics during the stepwise addition stage, a related least squares problem is solved.

We fitted a POLYCLASS model with 350 basis functions to the data. This maximum number was constrained by the computing resources that were available to us on a network of workstations at the Maui High Performance Computing Center. We believe that a larger number of basis functions would give better results. Exhaustion of our computing resources also prevented us from applying the stepwise deletion algorithm to the largest model. However, intermediate results suggest that the deletion of some basis functions would not significantly improve our results.

Of the 350 basis functions that were selected by the POLYMARS algorithm, 1 is the constant function, 31 are of the form x_i , 45 are of the form $(x_i - x_{ik})_+$, 134 are of the form $x_i x_j$, 87 are of the form $(x_i - x_{ik})_+ x_j$ and 11 are of the form $(x_i - x_{ik})_+ (x_j - x_{jl})_+$. Thus, of the 63 features, 32 are not used. Of the remaining 31, 10 are involved in all types of basis functions, 10 more are involved in all types of basis functions except for $(x_i - x_{ik})_+ (x_j - x_{jl})_+$ and 8 are involved in basis functions of the types x_i , $(x_i - x_{ik})_+$, $x_i x_j$ and $x_i (x_j - x_{jk})_+$. Finally, two features have basis functions of the types x_i , $(x_i - x_{ik})_+$ and $x_i x_j$ only, and one feature appears only linearly in the model.

The 63 features can be organized in a 9 (cepstral coefficients) \times 7 (time points) table. If we label the features from 1, for the feature that occurs only linearly, to 5, for the features that are involved in all types of basis functions, and we ignore the entries for the 32 features that are unused, we obtain Table 5. From this table we clearly see that the most important information is obtained from time points -3 (37.5 ms before the phoneme was spoken), 0 (when the phoneme is spoken) and 3 (37.5 ms after the phoneme was spoken). This table suggests that, in retrospect, it would have been better to use the cepstral coefficients at more than seven time points. (We also see that the log-gain and the shorter lags are more important than the longer lags.)

In Figure 3 we report the misclassification rate and the fitted log-likelihood

$$\frac{\sum_i \log P(Y = Y_i | \mathbf{X} = \mathbf{X}_i)}{n}$$

TABLE 5
The features in the POLYCLASS model

Cepstral Coefficient	Time						
	-3	-2	-1	0	1	2	3
Log-gain	5	4	3	5	3		
Lag 1	5		4	5			4
Lag 2	4		5	2			5
Lag 3	4			4			5
Lag 4	5			5	1		5
Lag 5	3			4			4
Lag 6				4			3
Lag 7	3		2				3
Lag 8	3		3				4

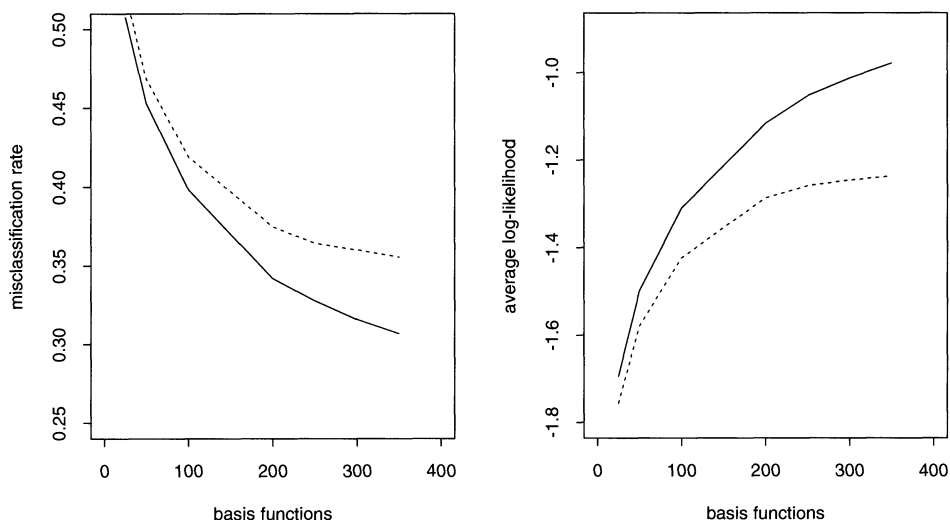


FIG. 3. Misclassification rate (left) and fitted log-likelihood (right) versus the number of basis functions. Solid line, training set; dashed line, test set.

for the training set and the test set combined. From these graphs it appears that the fit would continue to improve if we were to increase the number of basis functions.

As mentioned earlier, in this particular application the estimation of conditional class probabilities is more important than classification, since these probabilities can be used as inputs to the hidden Markov model for the approach to speech recognition described in Bourlard and Morgan (1994). POLYCLASS is particularly useful in this situation since, unlike most other classification methods, it provides viable estimates of the conditional class probabilities. In Figure 4 we plot the estimated probability that a case is a particular phoneme grouped in bins of size 0.01 on the horizontal axis and the fraction of cases with that probability that correspond to the correct phoneme on the vertical axis. Note that each case contributes 45 observations to this graph: one observation per candidate phoneme. These graphs are extremely close to the ideal straight line (fraction true class) = (estimated probability) for the test set (left side) and the training set (right side).

Clearly, not all phonemes are correctly estimated with the same probability. In Figure 5 we plot the average probability, over the test set, assigned to each phoneme. We see from Figure 5 that, not surprisingly, this probability is much larger for the frequently occurring phonemes than for the infrequently occurring ones.

Other aspects of the analysis that are discussed in Kooperberg, Bose and Stone (1997) are a comparison of POLYCLASS with other classification methods and an analysis of the patterns of misclassification by POLYCLASS. In

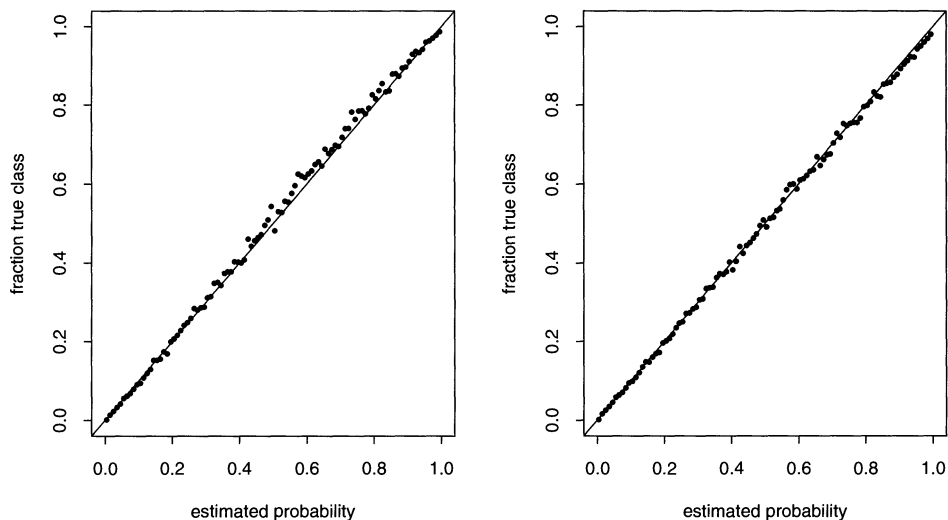


FIG. 4. Fraction of phonemes that correspond to the true class versus the estimated probability. Data have been grouped in bins of size 0.01. Left, training set; right, test set.

particular, it was found that most of the traditional classification methods either are not able to deal with such a large data set or are outperformed by POLYCLASS. Neural networks, however, do give better results on related, but not identical, data. It was hypothesized that for POLYCLASS to be competitive with neural networks it should be able to fit larger models faster, so

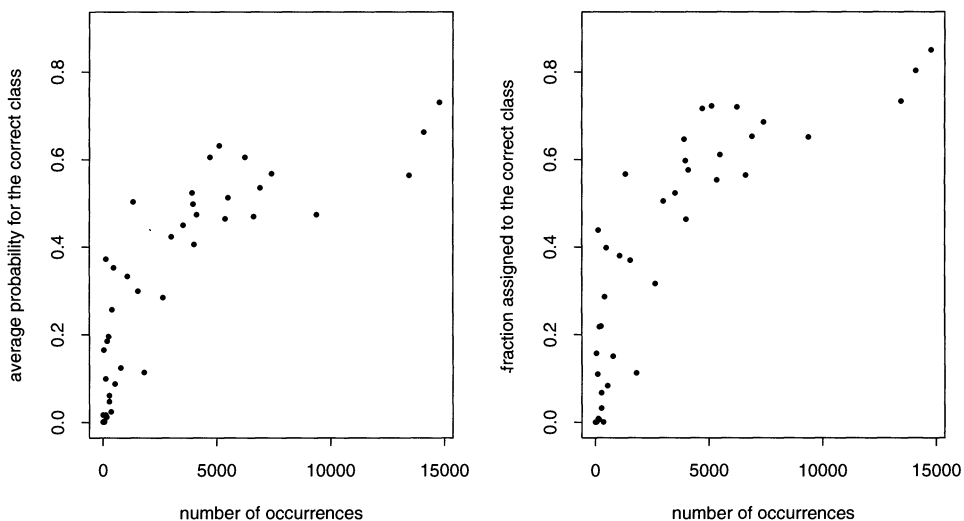


FIG. 5. Average probability assigned to the correct class and fraction correctly classified versus the class frequency for the test set.

that, for example, one could experiment with different sets of features. It may be that a stochastic gradient method (as in the backpropagation algorithm used in fitting neural networks) can give POLYCLASS the required computing power.

6.3. *Some more details of POLYCLASS.* The basis functions that are used in POLYCLASS are piecewise linear splines and their tensor products. We impose similar restrictions as in POLYMARS on which basis functions are allowed; that is, linear functions in one of the predictors are always allowed, while basis functions of the form $(x_i - x_{ik})_+$ are allowed in the model only when the corresponding linear function is already included in the model. Tensor products of basis functions involving two different predictors already in the model are allowed, except that if such a tensor product involves a knot in either or both of the predictors, the corresponding basis functions with linear terms must already be in the model. Thus, for $(x_i - x_{ik})_+(x_j - x_{jl})_+$ to be allowed in the model $x_i(x_j - x_{jl})_+$, $(x_i - x_{ik})_+x_j$ and x_ix_j need already be in the model.

The main difference between POLYCLASS and the other methodologies discussed in this paper is that in POLYCLASS there are K parameters for each basis function, while for the other methodologies there is only one parameter. This substantially increases the amount of computation needed for large data sets. For example, for the phoneme recognition problem discussed in the previous section the number of parameters for the largest model equals 15,400. Thus even storage of a (pseudo-) Hessian becomes prohibitively expensive, while the computation of one score function takes $O(JKn)$ floating point operations (flops) for a model with J basis functions and the computation of a Hessian takes $O(J^2K^2n)$ flops. The following modifications of the POLYCLASS algorithm, to make it feasible to deal with very large data sets, are discussed in Kooperberg, Bose and Stone (1997):

1. During the stepwise addition stage of the program we use a multiresponse least squares approximation to the POLYCLASS problem. That is, we regress $K + 1$ response vectors Z_k on the basis functions, where $Z_{ki} = \text{ind}(Y_i = k)$, $i = 1, \dots, n$ and $k = 1, \dots, K + 1$, with $\text{ind}(\cdot)$ being the usual indicator function. This least squares approximation can conveniently be carried out using a multiresponse version of the MARS algorithm described in Section 5. Selecting J basis functions now requires $O(50nJ(J + K))$ flops.
2. After the J basis functions have been selected using this least squares approximation, we immediately fit the largest model using maximum likelihood. To obtain good starting values we successively add basis functions to the model, using only a fraction of the cases, until all basis functions are in the model.
3. The code was modified to enable the maximum likelihood fitting to be carried out on a network of 64 workstations at the Maui High Performance Computing Center.

With these modifications, the time needed to fit the largest POLYCLASS model was reduced from an estimated several years to one day on the network of workstations.

7. Hazard regression. Recall the discussion of hazard regression in Section 2. Let $F(t|\mathbf{X}) = P(T \leq t|\mathbf{X})$ denote the conditional distribution function of the survival time T given the random vector \mathbf{X} of covariates and let $f(t|\mathbf{X})$ denote the corresponding conditional density function. Define the conditional hazard function by $\lambda(t|\mathbf{X}) = f(t|\mathbf{X})/[1 - F(t|\mathbf{X})]$ and set $\phi(t|\mathbf{X}) = \log \lambda(t|\mathbf{X})$. A proportional hazard model is specified by setting $\phi(t|\mathbf{X}) = \phi_0(t) + \mathbf{X}\boldsymbol{\beta}$; here $\phi_0(\cdot)$ is the baseline log-hazard function and $\boldsymbol{\beta} \in \mathbb{R}^M$ is a vector of parameters. Cox (1972) suggested a partial likelihood principle for estimating $\boldsymbol{\beta}$. Since then, analyses of censored outcome data have largely been confined to the estimation of linear covariate effects. See, for example, Andersen, Borgan, Gill and Keiding (1993), Cox and Oakes (1984), Fleming and Harrington (1991), Kalbfleisch and Prentice (1980) and Miller (1981).

The desire to relax the proportionality and linearity assumptions has led to many further developments in survival analysis. For example, Hastie and Tibshirani (1990), Sleeper and Harrington (1990) and Gray (1992) considered using splines to model nonlinear covariate effects in large clinical studies. In practice, it is even more desirable to estimate the conditional hazard, distribution and density functions. Based on proportional hazards models, Breslow (1972, 1974) suggested estimating the conditional distribution by combining Cox's partial likelihood principle for the covariate effects and the Kaplan and Meier (1958) method for estimating the baseline survival function. Following the extended linear modeling framework described in Sections 2 and 3, Kooperberg, Stone and Truong (1995a, b) developed a more general approach, which, without requiring the proportionality and linearity assumptions, yields estimates of the conditional hazard, density, survival and quantile functions in a unified manner using the relationships

$$F(t|\mathbf{x}) = 1 - \exp\left(-\int_0^t \lambda(u|\mathbf{x}) du\right) \quad \text{and} \quad f(t|\mathbf{x}) = [1 - F(t|\mathbf{x})]\lambda(t|\mathbf{x}), \quad t \geq 0.$$

In the remainder of this section, we describe the methodologies for hazard estimation with flexible tails (HEFT) and hazard regression (HARE), and we give an example to illustrate their practical application.

7.1. The HEFT and HARE methodologies.

HEFT. The HEFT methodology is designed to estimate the unconditional (or baseline) log-hazard function. Let f denote a positive density function on $(0, \infty)$ and let F , λ and ϕ be its distribution, hazard and log-hazard functions, respectively. Given the integer $J \geq 3$ and the sequence t_1, \dots, t_J with $0 < t_1 < \dots < t_J < \infty$, let G_0 be the $(J - 2)$ -dimensional space of twice continuously differentiable, cubic spline functions s on $[0, \infty)$ with knots t_1, t_2, \dots, t_J such that s is constant on $[0, t_1]$ and on $[t_J, \infty)$. Let B_1, \dots, B_{J-2} be a basis of this space such that $B_{J-2} = 1$ on $[0, \infty)$ and $B_1, \dots, B_{J-3} = 0$ on $[t_J, \infty)$.

To enhance its flexibility in estimating the hazard function, the space G_0 can be augmented by adding the basis functions

$$B_{-1}(t) = \log \frac{t}{t+c} \quad \text{and} \quad B_0(t) = \log(t+c), \quad t > 0,$$

with $c > 0$ being a parameter. In fact, the linear space G spanned by $G_0 \cup \{B_{-1}, B_0\}$ includes Weibull and Pareto distributions as special cases [see Kooperberg, Stone and Truong (1995a)]. The collection \mathcal{S} of such J -dimensional spaces G forms a family of allowable spaces.

Set

$$\begin{aligned} \boldsymbol{\beta} &= (\beta_{-1}, \beta_0, \beta_1, \dots, \beta_{J-2}) \in \mathbb{R}^J, \\ \phi(\cdot; \boldsymbol{\beta}) &= \beta_{-1}B_{-1}(\cdot) + \beta_0B_0(\cdot) + \beta_1B_1(\cdot) + \dots + \beta_{J-2}B_{J-2}(\cdot) \end{aligned}$$

and

$$\mathcal{B} = \{(\beta_{-1}, \beta_0, \beta_1, \dots, \beta_{J-2}) \in \mathbb{R}^J: \beta_{-1} > -1 \text{ and } \beta_0 \geq -1\}.$$

The above constraints ensure that $\int_0^t \exp \phi(u; \boldsymbol{\beta}) du < \infty$ for $0 < t < \infty$ and $\int_0^\infty \exp \phi(t; \boldsymbol{\beta}) dt = \infty$. We use $\phi(\cdot; \boldsymbol{\beta})$, $\boldsymbol{\beta} \in \mathcal{B}$, to model the log-hazard function.

Given a random sample, the maximum likelihood estimate $\hat{\boldsymbol{\beta}}$ of $\boldsymbol{\beta}$ is obtained by using the Newton–Raphson method. (Note that the log-likelihood function here is easily obtained from that for hazard regression discussed in Section 2 by ignoring the covariates.) Estimates of the log-hazard, hazard, survival, distribution and density functions are given by $\hat{\phi}(t) = \phi(\cdot; \hat{\boldsymbol{\beta}})$, $\hat{\lambda}(t) = \exp \hat{\phi}(t)$, $\hat{S}(t) = \exp(-\int_0^t \hat{\lambda}(u) du)$, $\hat{F}(t) = 1 - \hat{S}(t)$ and $\hat{f}(t) = \hat{S}(t)\hat{\lambda}(t)$, $t \geq 0$. The corresponding estimate of the p th quantile is given by $\hat{Q}_p = \hat{F}^{-1}(p)$.

Observe that the above log-hazard estimate depends on the choice of G . HEFT selects such a G adaptively from \mathcal{S} by following the methodology for model selection described in Section 3. (In the current implementation of HEFT, the choice of which logarithmic terms to include in the model is made initially by the user and is not modified during the process of stepwise addition and deletion of knots.)

HARE. HARE is a routine for estimating covariate effects on a possibly censored response variable. Here the allowable spaces are similar to those used in POLYMARS, except that the conditional log-hazard function also depends on time. To this extent we also allow piecewise linear basis functions depending on time and tensor products of these with (piecewise linear) basis functions depending on a covariate. As with POLYMARS and POLYCLASS, the highest order of interactions allowed is two. Let \mathcal{S} denote the collection of such allowable spaces.

For an allowable space in \mathcal{S} , we get estimates of the coefficients of basis functions by maximizing the log-likelihood function given in the discussion of hazard regression in Section 2. This procedure is carried out using the Newton–Raphson method. Estimates of the conditional log-hazard, conditional hazard, conditional survival, conditional distribution and conditional density functions are obtained in a manner similar to HEFT.

For model selection, the adaptive methodology is essentially the same as described in Section 3 with $d \leq 2$. In the current implementation of HARE, the fitted conditional log-hazard function has a constant tail. For details, see Kooperberg, Stone and Truong (1995a).

Besides providing a unified framework for estimating the conditional hazard, survival, density and quantile functions, HEFT and HARE also allow considerable flexibility in fitting survival data. If the fitted model contains an interaction involving time and a covariate, then the assumption of proportionality is questionable. On the other hand, HARE can be forced to fit a proportional hazards model or even an additive model ($d = 1$).

HEFT as preprocessor to HARE. Before applying HARE, it is useful to transform the time variable using HEFT. There are two advantages in doing this. First, because of the piecewise linear nature of HARE, the first derivative of the baseline hazard function can have big jumps at various knots in time. The HARE model for the transformed data, on the other hand, typically has fewer knots and the jumps in the first derivative of the hazard function at these knots tend to be smaller. Second, the fitted conditional hazard function beyond the last knot is necessarily constant when HARE is applied to the original data, but this is not the case when HARE is applied to the transformed values of time.

Let λ_0 denote the unconditional (baseline) hazard function of T and set $q_0 = -\log(1 - F_0)$ with F_0 being the distribution function corresponding to λ_0 , so that q_0 is the baseline cumulative hazard function. Then $q_0(T)$ has constant hazard function [see Kooperberg, Stone and Truong (1995a)]. This motivates the use of HARE on the transformed responses.

We next describe relationships between the transformed and untransformed data. Let f_1 , F_1 and λ_1 denote the conditional density, distribution and hazard functions of $q_0(T)$ given \mathbf{X} . Then the corresponding functions for T given \mathbf{X} are given, respectively, by

$$f(t|\mathbf{X}) = \lambda_0(t)f_1(q_0(t)|\mathbf{X}), \quad F(t|\mathbf{X}) = F_1(q_0(t)|\mathbf{X})$$

and

$$\lambda(t|\mathbf{X}) = \lambda_0(t)\lambda_1(q_0(t)|\mathbf{X}).$$

Moreover, the p th conditional quantile function is given by

$$Q_p(\mathbf{x}) = F^{-1}(p|\mathbf{x}) = q_0^{-1}(F_1^{-1}(p|\mathbf{x})).$$

Given a random sample, our methodology starts by applying HEFT to the response variables (no covariates), yielding an estimate $\hat{\lambda}_0$ of λ_0 . Then \hat{q}_0 is constructed based on the formula of the cumulative hazard function. Next the HARE methodology is applied to the transformed responses $\hat{q}_0(T)$, yielding an estimate $\hat{\lambda}_1$ of the conditional hazard function for the transformed data. Finally, we obtain estimates of the original conditional density, distribution, hazard and quantile functions using the relationships given above.

7.2. *An example.* In this section we use HEFT and HARE to analyze data from a clinical trial. The studies of left ventricular dysfunction [SOLVD (1990)] involves two double-blind, randomized clinical trials to test improved survival by treatment with enalapril, an inhibitor of angiotensin-converting enzyme, in patients with left ventricular dysfunction with or without congestive heart failure (CHF). The study started with a registry of 6273 patients involving 23 centers located in the United States, Canada and Belgium. Men and women aged 21–80 years with an ejection fraction (defined below) of at most 35% were eligible for the trials. In particular, patients with overt CHF were eligible for the treatment trial, whereas those with left ventricular dysfunction but no history of overt CHF were eligible for the prevention trail. Recruitment began in 1986, and the study terminated in 1991.

We will illustrate the use of HEFT and HARE on the treatment arm consisting of 2569 patients. Here the event is defined as death or hospitalization due to CHF. The response is time (in days). Among the 2569 observations, 1219 were censored. The censoring occurred when the patient was lost to follow-up or was still alive and never hospitalized due to CHF by the end of the study. We begin our analyses by applying HEFT to the possibly censored responses, yielding a model for the unconditional log-hazard function consisting of three knots and a log term (B_{-1}). Figure 6 shows estimates of the unconditional hazard and survival functions. As the right side of Figure 6 shows, our survival function estimate is remarkably close to the Kaplan–Meier estimate.

Next, HARE was applied to examine covariate effects on CHF. We used a set of 10 covariates: treatment (1=enalapril, 0=placebo); serum sodium level (serum); systolic blood pressure (SBP); diastolic blood pressure (DBP); smoking (1 = currently smoking, 0 = not currently smoking); sex (1 = female, 0 = male);

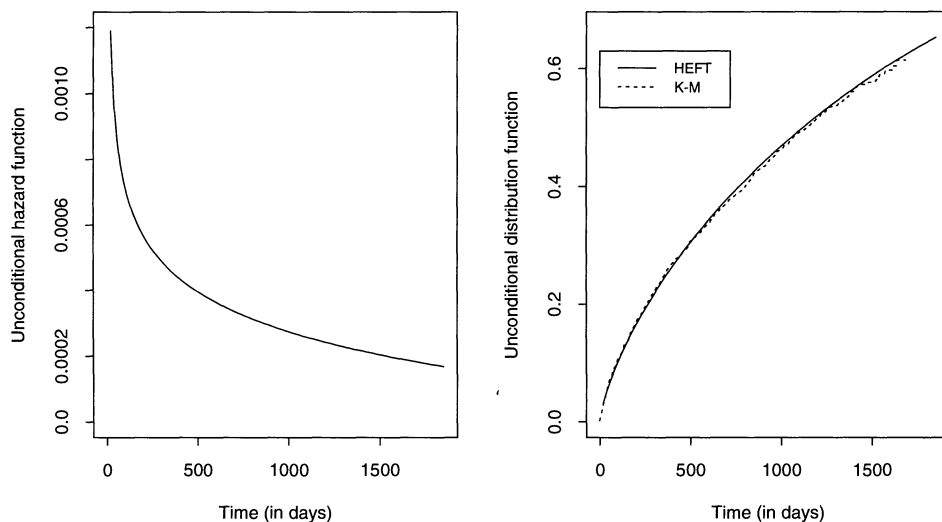


FIG. 6. *Estimated unconditional hazard and distribution functions using HEFT for the SOLVD data.*

age; adherence (a measure of treatment or placebo use in terms of numbers of pills taken and dispensed); New York Heart Association (NYHA) functional class I–IV (with I indicating the least severity of illness and IV indicating the greatest severity); and ejection fraction (EF).

The ejection fraction (EF) is the fraction (measured as a percentage) of the blood that is pumped from the left ventricle into the body's vascular system. After oxygenation in the lung, blood flows back to the left atrium of the heart and continues to the left ventricle. This is the chamber that "ejects" the blood from the heart into the body. Clearly, 100% of the blood cannot be ejected, but in normal hearts this fraction is at least 60%. In damaged hearts, where the muscle of the left ventricle is not working well (maybe from the effects of a previous heart attack), the fraction can be much lower, say 25–40%. Clinically, an EF of less than 35% is reason for concern. Below 15–20% the blood backs up into the atrium and lung, causing congestion and malfunctioning of the lung (CHF) and possibly death.

After removing the 69 cases with missing values on one or more covariates, we obtained a data set with 2500 observations and 1308 events. In our analyses we treated the covariate NYHA as an unordered categorical variable. Alternatively, we could have treated it as an ordinary variable having the four possible values 1, 2, 3 and 4.

Table 6 shows the results of applying HARE in various ways. Specifically, Model 1 summarizes the fit to the untransformed responses, which has 15

TABLE 6
*HARE analyses of the SOLVD data**

Basis Function	Model 1	Model 2	Model 3	Model 4
1	7.550	34.900	32.016	32.706
Age	0.013	0.010	0.009	0.011
Smoking	0.400			0.184
DBP		-0.424	-0.388	-0.400
EF	-0.567	-0.026	-0.026	-0.026
NYHA I			-0.294	-0.291
NYHA II	-0.462			
NYHA III	0.757	0.527	0.485	0.479
NYHA IV	1.210	0.980	18.577	19.004
Serum	-0.114	-0.248	-0.227	-0.233
Treatment	-0.124	-0.312	-0.302	-0.303
$(111 - t)_+$	0.006			
$(562 - t)_+$	0.002			
DBP \times serum		0.003	0.003	0.003
EF \times serum	0.004			
NYHA IV \times serum			-0.127	-0.130
$(562 - t)_+ \times$ smoking	-0.001			
$(562 - t)_+ \times$ NYHA II	0.001			
$(562 - t)_+ \times$ treatment	-0.001			
BIC	21,620.17	21,562.30	21,561.83	21,562.32

*See text for the model descriptions.

basis functions and $\widehat{\text{BIC}} = 21,620.17$. As discussed in Section 7.1, the above analysis can further be refined by applying HARE to the transformed responses using $\widehat{q}_0(t) = -\log(1 - \widehat{F}_0(t))$, where $\widehat{F}_0(t)$ is shown on the right side of Figure 6. This yields a proportional hazards model having nine basis functions with no knots and $\text{BIC} = 21,562.30$. (Actually, BIC for the transformed data is 2480.49. We used the relationships described in Section 7.1 to retrieve BIC for the untransformed data.) The resulting fit is referred to as Model 2 in Table 6. Note that all of the interactions and the two nonlinear terms involving time have disappeared; this may be explained by the nature of the transformation $\widehat{q}_0(T)$. While HARE models allow for nonlinearity, this smaller model is linear and easier to interpret. In general, one of the strengths of HARE is that it chooses more complicated models only when simpler ones do not fit nearly as well [see the examples in Kooperberg, Stone and Truong (1995a)].

HARE facilitates the visual examination of covariate effects. For example, Figure 7 shows estimates of the conditional hazard and survival functions for a patient having the covariate values given by

$$\begin{aligned} \text{treatment} = 1, \quad \text{serum sodium} = 138.95, \quad \text{EF} = 24.85, \\ \text{DBP} = 76.81, \quad \text{NYHA} = \text{IV}, \quad \text{smoking} = 1, \quad \text{age} = 60.88. \end{aligned}$$

These values were chosen to represent an average smoking, NYHA class IV, treated patient. Figure 7 also compares results from untransformed data (Model 1) and transformed data (Model 2). We remark that the estimated hazard function for the untransformed data exhibits a constant tail, as was

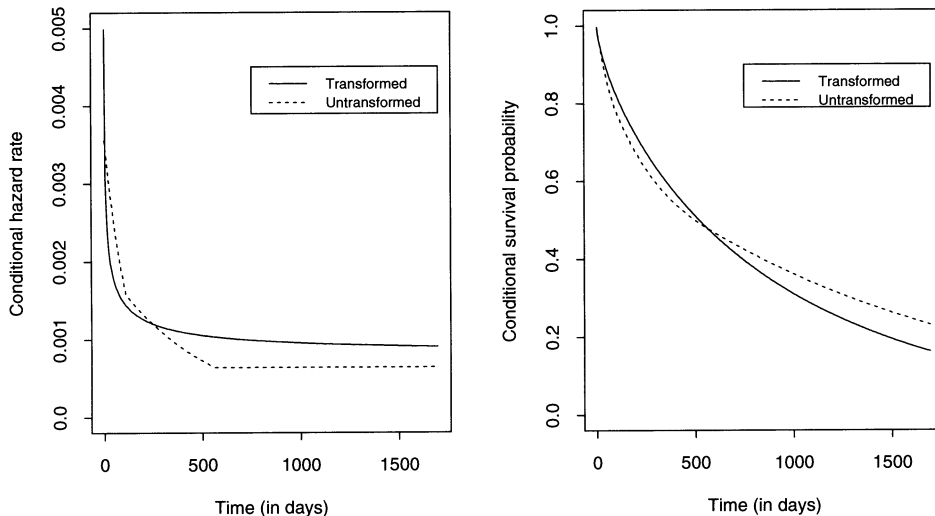


FIG. 7. Estimated conditional hazard and survival functions for an average smoking, NYHA class IV, treated patient using HARE for the SOLVD data.

discussed in Section 7.1. Estimates of the conditional density and quantile functions are also easily obtained using HARE.

We continue our analysis by using other options in HARE. Since Model 2 is a proportional hazards model, we decided to reapply HARE forcing it to fit such a model. Model 3 of Table 6 summarizes the resulting fit, indicating a slightly different proportional hazards model with 11 basis functions and $BIC = 21,561.83$. (BIC for the transformed data is 2480.01.) Comparing this model with Model 2, we note that HARE has reduced BIC slightly by including two more basis functions, NYHA I and NYHA IV \times serum.

For a further comparison, we fitted the transformed values of time and the same covariates as above using *coxreg* from S-PLUS. In light of the analysis using HARE, we forced the two interaction terms of Model 3 into the Cox model (the default form of *coxreg* estimates main effects only). Table 7 provides a summary of the fit.

Observe that the interaction terms are highly significant and that the fit is similar to Model 3, except that the covariate smoking is significant and the constant term is not allowed in *coxreg*. Since there is no knot in Model 3, we felt that the default penalty value $\log(2500) \doteq 7.82$ of HARE might have been too high. (This is equivalent to using the chi-squared test with 1 degree of freedom and the significance level of $\alpha \doteq 0.005$ to test the model with 12 basis functions versus a submodel with 11 basis functions.) By using a smaller penalty value of 7.1 ($\alpha \doteq 0.007$) and refitting the data using HARE, we obtained Model 4 in Table 6, which has 12 basis functions. This model is in close agreement with the one obtained by using *coxreg* and shown in Table 7. Moreover, the standard errors of the coefficients in Model 4 (not shown) are remarkably close to the corresponding ones in Table 7. We conclude that Model 4 is our most reasonable HARE model for the data.

Note that the treatment effect is included in all five models discussed above. In fact, the treatment was so effective that, for ethical reasons, the trial was terminated early. Other important covariates are the ejection fraction

TABLE 7
Analyses of the SOLVD data using coxreg from S-PLUS

Variable	Coefficient	SE	P-value
Age	0.011	0.003	0.000
Smoking	0.185	0.067	0.006
DBP	-0.401	0.106	0.000
EF	-0.027	0.004	0.000
NYHA I	-0.293	0.106	0.005
NYHA III	0.479	0.059	0.000
NYHA IV	19.480	6.040	0.001
Serum	-0.234	0.061	0.000
Treatment	-0.304	0.056	0.000
DBP \times serum	0.003	0.001	0.000
NYHA IV \times serum	-0.134	0.044	0.002

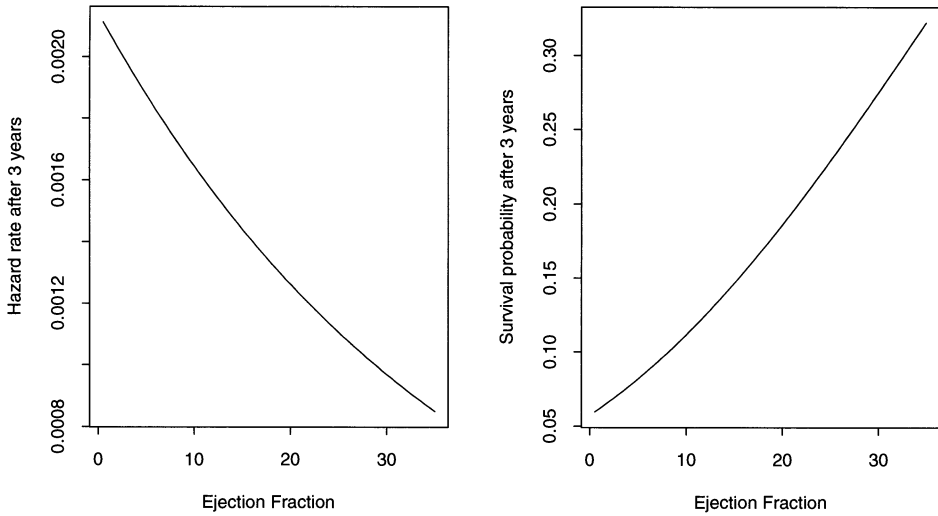


FIG. 8. *Left side: estimated conditional hazard rate after 3 years as a function of EF. Right side: estimated conditional survival probability after 3 years as a function of EF. Same covariates as in Fig. 7.*

(EF), age and the NYHA functional class. To demonstrate another strength of HARE, we use Model 4 to examine graphically some of the above covariate effects. Figure 8 illustrates estimates of the conditional hazard rate and survival probability after 3 years as a function of EF. We see that the hazard rate decreases and the survival probability increases with EF. Figure 9 shows

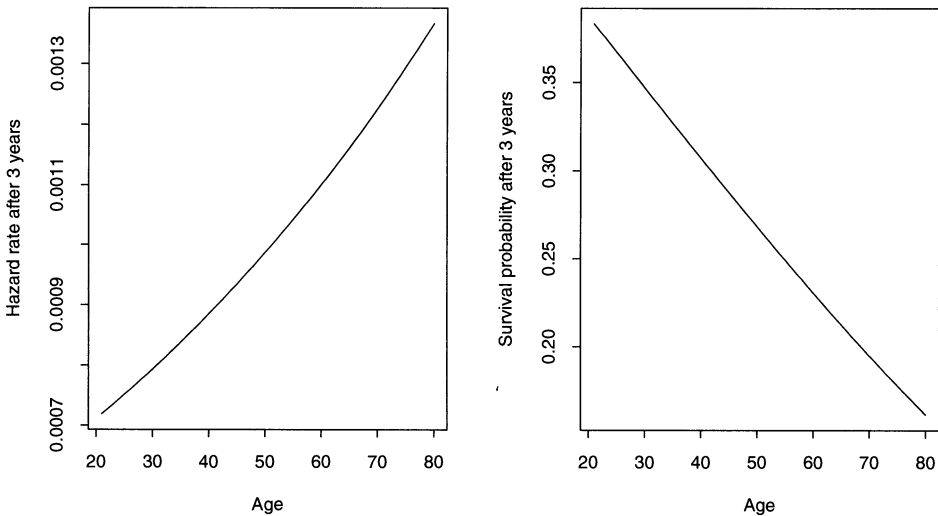


FIG. 9. *Left: Estimated conditional hazard rate after 3 years as a function of age. Right: Estimated conditional survival probability after 3 years as a function of age. Same covariates as in Figure 7.*

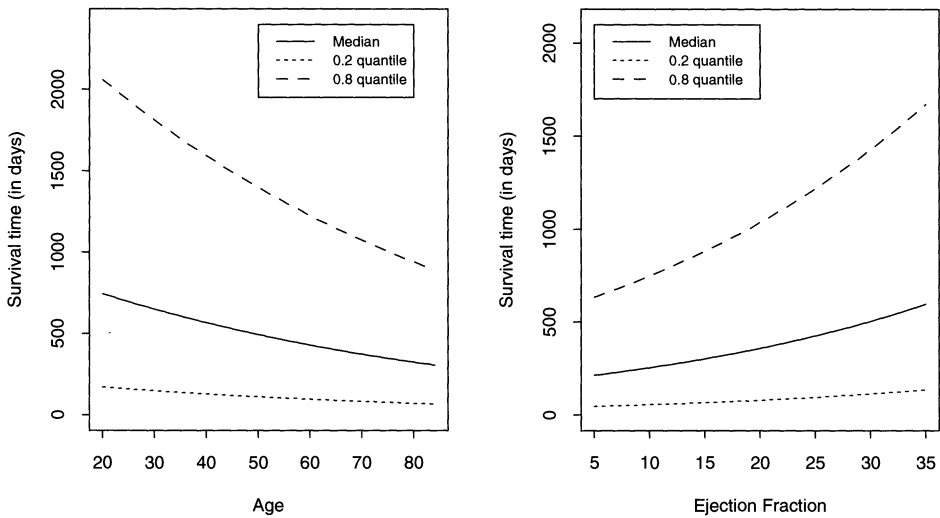


FIG. 10. *Estimated conditional quantile functions based on Model 4 as a function of age (left) and as a function of EF (right). Same covariates as in Figure 7.*

estimates of the hazard rate and survival probability after 3 years as functions of age. It is observed that older participants have a higher risk than younger ones.

As a final illustration of HARE, Figure 10 shows estimates of the 20th, 50th and 80th percentiles as functions of age and EF based on Model 4. Observe that the median survival time decreases with age, while it increases with EF.

In summary, in the above analyses the HEFT and HARE methodologies yielded estimates of the (conditional) hazard, survival, density and quantile functions in a consistent manner without requiring the proportionality assumption. Moreover, our highly adaptive methodology performs well in comparison with the traditional approach even when that approach is applicable. In light of this example and those given in Kooperberg, Stone and Truong (1995a), we find that HEFT and HARE are useful tools for survival analysis.

8. Spectral analysis. For stationary time series, it is known that the periodogram ordinates at the Fourier frequencies are approximately independent and have an exponential distribution with mean equal to the spectral density function. This implies that the periodogram is not a consistent estimate, but consistency can be achieved by smoothing the periodogram ordinates [see Brillinger (1981)]. In this section we present our version of the spectral estimate by treating it as a special case of the generalized regression problem discussed in Section 2. Specifically, we use the theory and methodology of extended linear models to estimate the logarithm of the mean of the exponential distribution function. Here the mean is the spectral density function.

To describe the possibly mixed spectral distribution, consider a real-valued, second-order stationary time series X_t with mean $E(X_t) = E(X_0)$ and covariance function $\gamma(u) = \text{cov}(X_t, X_{t+u})$. Assume that the time series has the form

$$X_t = \sum_{j=1}^p R_j \cos(t\lambda_j + \varphi_j) + Y_t.$$

Here $0 < \lambda_j \leq \pi$; φ_j are independent and uniformly distributed on $[-\pi, \pi]$; R_j are independent, nonnegative random variables such that R_j^2 has positive mean $4\rho_j$; and Y_t is a second-order stationary time series with $E(Y_t) = E(X_0)$ and autocovariance function $\gamma_c(u) = \text{cov}(Y_t, Y_{t+u})$ satisfying $\sum_u |\gamma_c(u)| < \infty$.

The spectral distribution function of X_t is given by

$$F(\lambda) = \int_{-\pi}^{\lambda} f_c(\omega) d\omega + \sum_{\omega \leq \lambda} f_d(\omega), \quad |\lambda| \leq \pi,$$

where

$$f_c(\lambda) = \frac{1}{2\pi} \sum_{u=-\infty}^{\infty} \gamma_c(u) \exp(iu\lambda), \quad |\lambda| \leq \pi,$$

and

$$f_d(\lambda) = \begin{cases} \rho_j, & \text{if } \lambda = \pm\lambda_j, \\ 0, & \text{otherwise.} \end{cases}$$

The functions f_c and f_d are referred to as the *spectral density function* and *line spectrum* of the time series X_t .

Note that f_c and f_d are nonnegative and symmetric about zero and that they can be extended to periodic functions on $(-\infty, \infty)$ with period 2π . From now on we limit our attention to the interval $[0, \pi]$. Observe that if the indicated derivatives of f_c exist, then $f'_c(0)$, $f'''_c(0)$, $f'_c(\pi)$ and $f'''_c(\pi)$ all equal zero.

8.1. *The LSPEC methodology.* Let $\delta_a(\lambda)$ equal 1 or 0 according as $\lambda = a$ or $\lambda \neq a$. Given a time series X_1, X_2, \dots, X_{T-1} , set $f = f_c + (T/2\pi)f_d$, $\phi = \log f$ and $\phi_c = \log f_c$. Then $\phi = \phi_c + \phi_d$, where $\phi_d = \beta_1\delta_{\lambda_1} + \dots + \beta_p\delta_{\lambda_p}$ with $\beta_1, \dots, \beta_p > 0$. Moreover, $f_d = (2\pi/T)(\exp \phi_d - 1)f_c$. In the following discussion, we will use cubic splines to obtain a finite-dimensional approximation to ϕ_c and hence to ϕ .

First, we describe the space of splines that will be used to model the logarithm of the spectral density function. Given the positive integer J_c , let G_c be the J_c -dimensional space of twice continuously differentiable, cubic spline functions s with the knot sequence $0 \leq t_1 < \dots < t_{J_c} \leq \pi$. We require that $s'(0) = s'(\pi) = 0$. Also, $s'''(0) = 0$ unless $t_1 = 0$, and $s'''(\pi) = 0$ unless $t_{J_c} = \pi$. Let B_1, \dots, B_{J_c} be a basis of G_c . Then functions in G_c can be extended to splines on $(-\infty, \infty)$ that are symmetric about zero, periodic with period 2π ,

have a knot at zero if and only if $t_1 = 0$ and have a knot at π if and only if $t_{J_c} = \pi$.

Next, we describe the space that will be used indirectly to model the line spectrum. Given the nonnegative integer J_d and the increasing sequence a_1, \dots, a_{J_d} of members of $\{2\pi j/T: 1 \leq j \leq T/2\}$, let G_d be the J_d -dimensional space of nonnegative functions s on $[0, \pi]$ such that $s = 0$ except at a_1, \dots, a_{J_d} . Set $B_{j+J_c}(\lambda) = \delta_{a_j}(\lambda)$ for $1 \leq j \leq J_d$. Then B_{J_c+1}, \dots, B_J form a basis of G_d , where $J = J_c + J_d$.

Let G be the space spanned by B_1, \dots, B_J . The collection \mathcal{S} of such J -dimensional spaces G forms a family of allowable spaces. Set

$$\phi_c(\cdot; \beta_c) = \beta_1 B_1(\cdot) + \dots + \beta_{J_c} B_{J_c}(\cdot), \quad \beta_c = (\beta_1, \dots, \beta_{J_c}) \in \mathbb{R}^{J_c},$$

$$\phi_d(\cdot; \beta_d) = \beta_{J_c+1} B_{J_c+1}(\cdot) + \dots + \beta_J B_J(\cdot),$$

$$\beta_d = (\beta_{J_c+1}, \dots, \beta_J) \quad \text{with } \beta_{J_c+1}, \dots, \beta_J \geq 0,$$

and

$$\phi(\cdot; \beta) = \phi_c(\cdot; \beta_c) + \phi_d(\cdot; \beta_d), \quad \beta = (\beta_1, \dots, \beta_J).$$

We use $\phi_c(\cdot; \beta_c)$ to model the logarithm of the spectral density function and $\phi(\cdot; \beta)$ to model $\log f$. Thus, $f_c(\cdot; \beta_c) = \exp \phi_c(\cdot; \beta_c)$, $f(\cdot; \beta) = \exp \phi(\cdot; \beta)$ and

$$f_d(\cdot; \beta_d) = \frac{2\pi}{T} [\exp \phi_d(\cdot; \beta_d) - 1] f_c(\cdot; \beta_c).$$

Denote the Fourier frequencies by $\lambda_k = 2\pi k/T$ for $k = 0, 1, \dots, [T/2]$. Let I_k denote the k th ordinate of the periodogram, which is given by

$$I_k = I^{(T)}(\lambda_k) = (2\pi T)^{-1} \left| \sum_{t=0}^{T-1} \exp(-i\lambda_k t) X_t \right|^2.$$

For Gaussian time series, I_k , $1 \leq k \leq [T/2]$, are independent and have the exponential distribution with mean equal to $f(\lambda_k) = \exp \phi(\lambda_k)$. Hence, the log-likelihood function is given by

$$l(\beta) = \frac{1}{[T/2]} \sum_{k=1}^{[T/2]} \left(\frac{\delta_\pi(\lambda_k)}{2} - 1 \right) [\phi(\lambda_k; \beta) + I_k \exp(-\phi(\lambda_k; \beta))], \quad \beta \in \mathbb{R}^J.$$

Observe that the log-likelihood is a concave function of β .

Let $\hat{\beta}$ denote the maximum likelihood estimate of β , which is obtained as usual by the Newton-Raphson method. The corresponding estimate of the function f is given by $\hat{f}(\lambda) = f(\lambda; \hat{\beta})$. Similarly, estimates of the spectral density function and line spectrum are given by $\hat{f}_c(\cdot) = f_c(\cdot; \hat{\beta}_c)$ and $\hat{f}_d(\cdot) = f_d(\cdot; \hat{\beta}_d)$, where $\hat{\beta}_c = (\hat{\beta}_1, \dots, \hat{\beta}_{J_c})$ and $\hat{\beta}_d = (\hat{\beta}_{J_c+1}, \dots, \hat{\beta}_J)$.

As in other cases discussed in this paper, our spectral estimate depends on G . We follow the procedure described in Section 3 (with $d = 1$) to select G adaptively from \mathcal{S} . This methodology is referred to as LSPEC in Kooperberg, Stone and Truong (1995c). (In the current implementation of LSPEC, if an

atom has a frequency that is not of the form $2\pi k/T$, then it is typically replaced by the two closest adjacent atoms with frequencies of this form. Also, LSPEC prevents atoms with small mass from entering the model.)

In the absence of atoms, the rate of convergence of the maximum likelihood estimate $\hat{\phi}_c$ is given in Kooperberg, Stone and Truong (1995d). This result lends theoretical support to LSPEC.

8.2. An example. We will use LSPEC to analyze the result of a neurophysiological experiment consisting of 30 trials of electrical potential (EP) measurements [see Durka, Kelly and Blinowska (1995)]. It started with a 24 Hz (cycles/s), 500 μm peak-to-peak sinusoidal stimulus applied to the right fingertip. The responses are the EP measurements at the scalp and wrist. Each EP measurement lasted for 6 s, with the stimulus coming on at 2 s and staying on for the remainder of the trial. The channels were sampled at 256 times/s, giving a total of 1536 sampling points per channel.

Since the stimulus was not active for the first 2 s, our analyses were based on the last 4 s of recordings, so that $T = 1024$. Figure 11 shows the averages of 30 EP responses from the scalp and wrist, which appear to be stationary. The left side of Figure 12 shows the LSPEC estimate of the scalp EP spectrum. We observe two lines with frequencies of 9.25 and 9.75 Hz [the former frequency corresponds to $k = 4(9.25) = 37$ and $\lambda = 2\pi(37)/1024 \doteq 0.227$, and the latter frequency corresponds to $k = 39$ and $\lambda \doteq 0.239$]. These are approximately the alpha-rhythm frequencies. There is also a peak with a frequency of 48 Hz ($\lambda \doteq 1.178$), corresponding to the second harmonic of the stimulus frequency 24 Hz. In the right side of Figure 12, we observe that the wrist EP responded with a

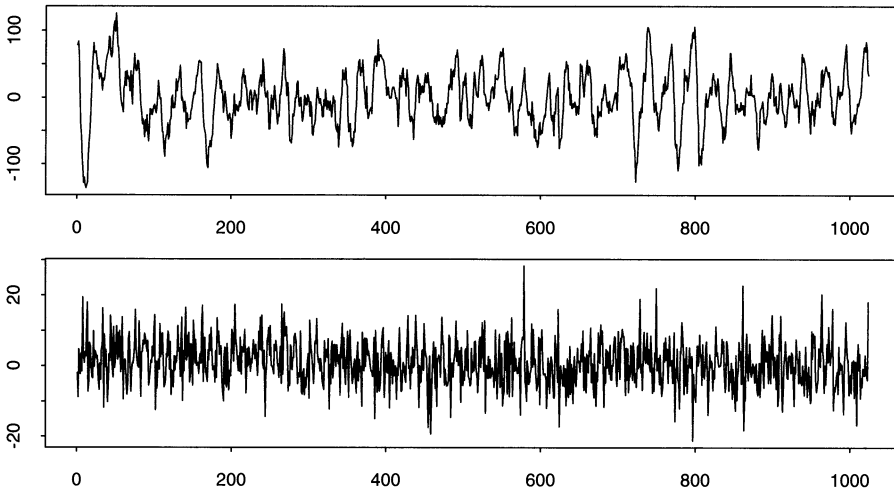


FIG. 11. Averages of 30 series of electrical potential (EP) measurements from the scalp (top) and wrist (bottom).

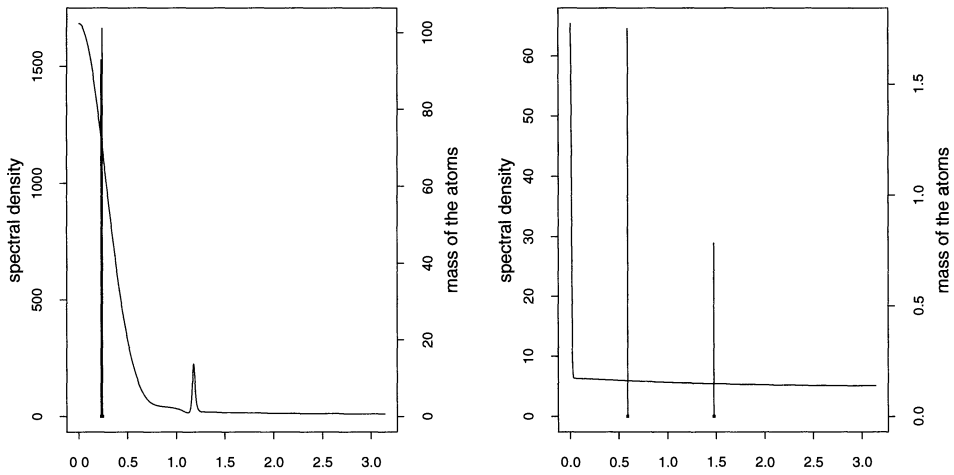


FIG. 12. The scalp EP spectrum (left) has line frequencies equal to 9.25 and 9.75 Hz; the peak has a frequency equal to 48 Hz. The line frequencies of the wrist EP spectrum (right) are 24 and 60 Hz.

frequency (the first line) at 24 Hz, while it also picked up the electrical power line frequency at 60 Hz. Note that the background noise level (the continuous spectrum) is much higher in the scalp EP than in the wrist EP.

The responses were then filtered to remove the unwanted (alpha-rhythm, electrical power line) signals and low frequency components of background noise, and sampled at 128 times/s, yielding a total of 512 sampling points. Applications of LSPEC to the filtered observations are illustrated in Figure 13.

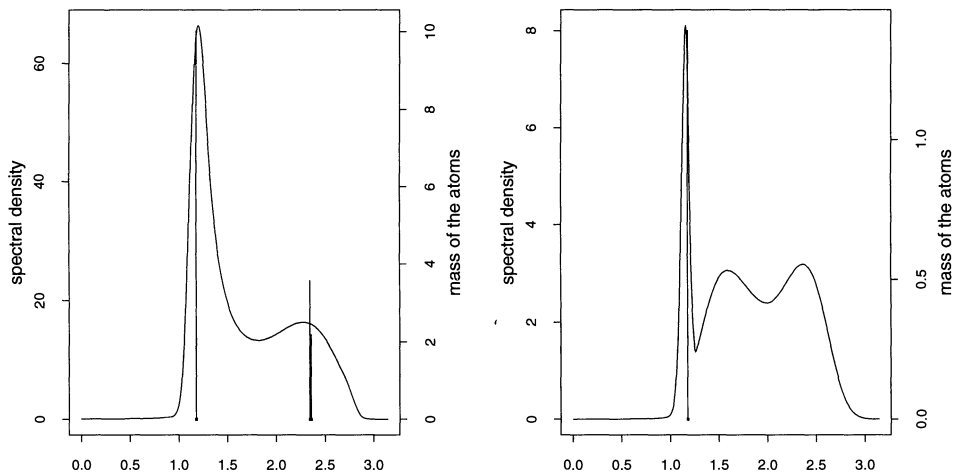


FIG. 13. Spectra of the filtered EP data. The scalp (left) has line frequencies equal to 24 and 48 Hz. The wrist (right) has a line frequency equal to 24 Hz.

For the scalp EP data, the resulting fit is a spline with seven knots and three lines in the model. The first line has a frequency of 24 Hz ($\lambda \doteq 1.178$), showing that LSPEC has located the desired signal. The other two lines correspond to the second harmonic. The fit for the wrist EP data shows a spline with eight knots and one line (at 24 Hz) in the model.

In summary, in this example the LSPEC methodology yielded a precise estimate of the stimulus frequency (24 Hz) and provided an informative description of the neurophysiological data. More generally, in the light of the present example and those given in Kooperberg, Stone and Truong (1995c), we find the LSPEC methodology to be both effective and of considerable practical value.

9. Models based on multivariate splines. In the last two decades, a considerable body of literature on multivariate spline spaces has been amassed by approximation theorists, numerical analysts and computer scientists. In this section, we demonstrate the practicality of these tools for statistical applications. We begin our survey on a theoretical note, developing rates of convergence for ANOVA decompositions based on multivariate splines and their tensor products. Then we shift our emphasis somewhat and consider techniques for adaptively constructing multivariate spline spaces, borrowing heavily from the ideas of knot addition and deletion presented in previous sections. Finally, we present a simple illustrative application of these ideas to bivariate logspline density estimation.

9.1. The extended linear model revisited. In Section 2, we introduced the notion of a concave extended linear model and discussed a variety of statistical problems that can be treated effectively within this framework. In each of these cases, our data consist of a sample from the distribution of a random vector \mathbf{W} . In this section, we focus our attention on the derived variable \mathbf{U} , which is typically a subvector of \mathbf{W} . Broadly speaking, we are interested in estimating a (possibly) vector-valued function $\phi^* = (\phi_1^*, \dots, \phi_K^*)$, where the constituents ϕ_k^* , $1 \leq k \leq K$, are real-valued functions on a set $\mathcal{U} = \mathcal{U}_1 \times \dots \times \mathcal{U}_M$, the range of \mathbf{U} . So far, we have considered only the case in which each of the sets $\mathcal{U}_1, \dots, \mathcal{U}_M$ is (in theory) a compact interval with positive length. Under this restriction, we are naturally led to estimators of ϕ^* that are built up from univariate spline spaces defined on these intervals. From a methodological perspective, however, tensor products of univariate splines may not be flexible enough to capture all of the features exhibited by a particular data set. In addition, known structural relationships between the variables that constitute \mathbf{U} might suggest that the domain of ϕ^* is something other than a hyperrectangle.

In the rest of our discussion, we allow $\mathcal{U}_1, \dots, \mathcal{U}_M$ to be compact subsets of $\mathbb{R}^{d_1}, \dots, \mathbb{R}^{d_M}$, respectively. In this case, the unknown function $\phi^* = \phi^*(u_1, \dots, u_M)$ is still defined on $\mathcal{U} = \mathcal{U}_1 \times \dots \times \mathcal{U}_M$, with the distinction that now the individual variables u_m may be vectors. Recall that our approach to estimating $\phi^* \in H^K$ begins with an ANOVA decomposition $\phi^* = \sum_{s \in \mathcal{S}} \phi_s^*$ that decomposes ϕ^* into its components ϕ_s^* , $s \in \mathcal{S}$. A parallel construction

is then used to define an ANOVA decomposition of the maximum likelihood estimate $\widehat{\phi} = \sum_{s \in \mathcal{S}} \widehat{\phi}_s$ in a space G^K consisting of smooth, piecewise polynomials. Not surprisingly, this approach can successfully be applied to derive the convergence properties of $\widehat{\phi}$ even when we allow the sets $\mathcal{U}_1, \dots, \mathcal{U}_M$ to be more complicated than compact intervals of the real line. Once we remove these restrictions, the components $\widehat{\phi}_s, s \in \mathcal{S}$, of the ANOVA decomposition of $\widehat{\phi}$ become *multivariate splines* and their tensor products.

To be more specific, for $1 \leq m \leq M$, let Δ_m be a partition of $\mathcal{U}_m \subset \mathbb{R}^{d_m}$ into disjoint (measurable) sets and for simplicity assume that each set has a common diameter a . By a piecewise polynomial of degree q over Δ_m , we now mean a function g on \mathcal{U}_m such that the restriction of g to each set $\delta \in \Delta_m$ is a polynomial of degree q in the d_m variables that constitute u_m . Let G_m be a linear space of *multivariate splines*; that is, piecewise polynomials of degree q on \mathcal{U}_m that satisfy certain smoothness constraints. Following the development in Section 2, for each $s \in \mathcal{S}$, we let G_s denote the tensor product of the spaces $G_m, m \in s$.

The rate at which $\widehat{\phi}$ and its components approach ϕ^* and its components were derived in Hansen (1994). In the simple case described so far, if we assume that the spaces G_s are flexible enough to ensure that

$$\inf_{g \in G_s} \|g - \phi_{ks}^*\|_\infty = O(a^p), \quad 1 \leq k \leq K \text{ and } s \in \mathcal{S},$$

where p is a measure of smoothness of the constituents of ϕ^* , we find that

$$\|\widehat{\phi}_s - \phi_s^*\|^2 = O_P\left(a^{2p} + \frac{1}{na^d}\right), \quad s \in \mathcal{S},$$

and

$$\|\widehat{\phi} - \phi^*\|^2 = O_P\left(a^{2p} + \frac{1}{na^d}\right),$$

where $d = \max_{s \in \mathcal{S}} \sum_{m \in s} d_m$. As we collect more and more data, if the sets in our partition shrink so that $a \sim n^{-1/(2p+d)}$, then we obtain the rates in (2.3) and (2.4) with the indicated definition of d . Hansen (1994) extended these results and, in particular, derived L_2 rates of convergence for the case when the various constituents ϕ_s^* satisfy different smoothness conditions and the sets in the triangulations Δ_m do not share a common diameter.

9.2. Bivariate splines and the extended linear model. For simplicity, we now focus our discussion on saturated, bivariate models, where $\phi^* = \phi$. Assume that \mathcal{U} is a compact region in the plane so that ϕ is a function of $\mathbf{u} \in \mathbb{R}^2$. In the context of our previous discussion, we now view \mathbf{U} as a single variable and hence will not attempt to decompose ϕ into components based on individual spatial coordinates. In the remaining pages, we will discuss the use of bivariate splines to construct estimates of ϕ .

Triangulations and piecewise linear basis functions. Let Δ be a collection of closed subsets of \mathcal{U} having disjoint interiors and satisfying $\mathcal{U} = \bigcup_{\delta \in \Delta} \delta$. In

general, the set Δ is a tessellation of \mathcal{U} . If each element $\delta \in \Delta$ is a triangle, Δ is said to form a triangulation of \mathcal{U} . Furthermore, a triangulation Δ is said to be *conforming* if the nonempty intersection between pairs of triangles in Δ consists of either a single shared vertex or an entire common edge (see Figure 14). Throughout this section, we reserve the symbol Δ for this special type of tessellation.

Given such a conforming triangulation Δ , we let G denote the space of continuous, piecewise linear functions over Δ . There is a natural association between the vertices $\mathbf{v}_1, \dots, \mathbf{v}_j$ of the triangles in Δ and the basis functions $B_1(\mathbf{u}), \dots, B_j(\mathbf{u})$ of G . To be more precise, we define $B_j(\mathbf{u})$ to be the unique function that is linear on each of the triangles in Δ and takes on the value 1 at \mathbf{v}_j and 0 at the remaining vertices in the partition. This collection of tent functions is frequently used in the finite element method and is often the starting point for defining multivariate splines of higher degrees [see Chui (1988), de Boor (1987) and Farin (1986)].

Many of the important properties of this basis can be obtained from a local representation of the tent functions. For the moment, consider a single triangle $\delta \in \Delta$ having vertices $\mathbf{v}_1, \mathbf{v}_2$ and \mathbf{v}_3 . Relative to δ , the *barycentric coordinates* of any point $\mathbf{u} = (u_1, u_2) \in \mathbb{R}^2$ are defined as a triple $\varphi(\mathbf{u}) = (\varphi_1(\mathbf{u}), \varphi_2(\mathbf{u}), \varphi_3(\mathbf{u}))$ such that

$$\mathbf{u} = \varphi_1(\mathbf{u})\mathbf{v}_1 + \varphi_2(\mathbf{u})\mathbf{v}_2 + \varphi_3(\mathbf{u})\mathbf{v}_3 \quad \text{and} \quad \varphi_1(\mathbf{u}) + \varphi_2(\mathbf{u}) + \varphi_3(\mathbf{u}) = 1.$$

Casting these conditions into a simple set of linear equations we find that

$$(9.1) \quad \begin{pmatrix} v_{11} & v_{21} & v_{31} \\ v_{12} & v_{22} & v_{32} \\ 1 & 1 & 1 \end{pmatrix} \begin{pmatrix} \varphi_1(\mathbf{u}) \\ \varphi_2(\mathbf{u}) \\ \varphi_3(\mathbf{u}) \end{pmatrix} = \begin{pmatrix} u_1 \\ u_2 \\ 1 \end{pmatrix}.$$

Provided that δ has a nonempty interior, this system can be solved explicitly, and the solution is best written in terms of the function $\text{SignedArea}(\mathbf{v}_1, \mathbf{v}_2, \mathbf{v}_3)$,

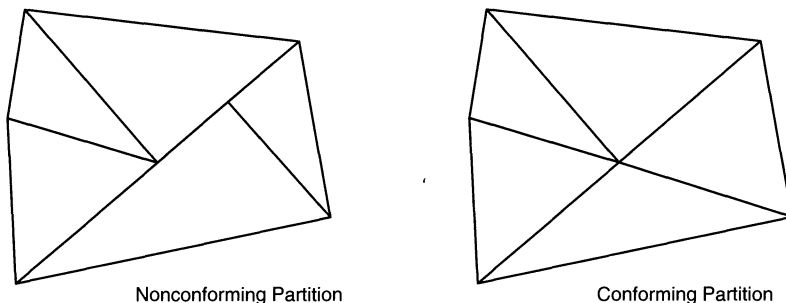


FIG. 14. In a nonconforming partition, at least one vertex of a triangle in Δ falls along the interior of an edge of another triangle in the partition.

which we define by

$$\text{SignedArea}(\mathbf{v}_1, \mathbf{v}_2, \mathbf{v}_3) = \frac{1}{2} \begin{vmatrix} v_{11} & v_{21} & v_{31} \\ v_{12} & v_{22} & v_{32} \\ 1 & 1 & 1 \end{vmatrix}.$$

As its name suggests, the absolute value of $\text{SignedArea}(\mathbf{v}_1, \mathbf{v}_2, \mathbf{v}_3)$ is just the area of the triangle with vertices \mathbf{v}_1 , \mathbf{v}_2 and \mathbf{v}_3 . By applying Cramér's method to the set of equations (9.1) we find that $\varphi_1(\mathbf{u})$ is given by the ratio

$$(9.2) \quad \varphi_1(\mathbf{u}) = \varphi_1(u_1, u_2) = \frac{\text{SignedArea}(\mathbf{u}, \mathbf{v}_2, \mathbf{v}_3)}{\text{SignedArea}(\mathbf{v}_1, \mathbf{v}_2, \mathbf{v}_3)}.$$

Thus, the barycentric coordinates are linear functions of u_1 and u_2 , where $\mathbf{u} = (u_1, u_2)$, and satisfy the interpolation conditions

$$(9.3) \quad \varphi_i(\mathbf{v}_j) = \begin{cases} 0, & i \neq j, \\ 1, & i = j, \end{cases} \quad i, j = 1, 2, 3;$$

hence the vertices \mathbf{v}_1 , \mathbf{v}_2 and \mathbf{v}_3 have barycentric coordinates $(1, 0, 0)$, $(0, 1, 0)$ and $(0, 0, 1)$, respectively. Furthermore, from (9.2) we see that the points on the edge connecting \mathbf{v}_2 and \mathbf{v}_3 have barycentric coordinates of the form $(0, \alpha, 1-\alpha)$, $\alpha \in [0, 1]$.

Given the interpolation conditions (9.3) and the consequence of (9.2) that the barycentric coordinate functions are linear functions of \mathbf{u} , we now have an explicit representation of the basis functions of G that correspond to the vertices of δ ; that is, for all $\mathbf{u} \in \delta$, $B_i(\mathbf{u}) = \varphi_i(\mathbf{u})$, $i = 1, 2, 3$. As an immediate consequence of this local (triangle by triangle) representation, we find that the basis functions B_1, \dots, B_J associated with the triangulation Δ are bounded between 0 and 1 and satisfy

$$B_1(\mathbf{u}) + \dots + B_J(\mathbf{u}) = 1, \quad \mathbf{u} \in \mathcal{U}.$$

From (9.2) it is also possible to demonstrate that, for any nonsingular, 2-by-2 matrix A and any vector $\mathbf{b} \in \mathbb{R}^2$,

$$B_j(\mathbf{u}) = B_j^*(A\mathbf{u} + \mathbf{b}), \quad \mathbf{u} \in \mathbb{R}^2,$$

where B_1^*, \dots, B_J^* is the basis associated with vertices $A\mathbf{v}_1 + \mathbf{b}, \dots, A\mathbf{v}_J + \mathbf{b}$ of the transformed set $\mathcal{U}^* = \{A\mathbf{u} + \mathbf{b}, \mathbf{u} \in \mathcal{U}\}$. This means that models built from functions in G have a natural invariance under affine transformations. Using the barycentric coordinate functions, we will see in the next subsection that this invariance carries over to our adaptive methodology as well.

To summarize, we have derived some of the essential properties of a basis for the space of continuous, piecewise linear functions associated with a triangulation Δ of \mathcal{U} . An important observation here is that there is a simple correspondence between the structure of the partition Δ and the basis functions of G . As in the previous sections, this relationship will allow us to use simple model selection criteria to construct a functional form of our estimate $\hat{\phi}$ of the unknown function ϕ . The only issue left to resolve is how we generalize the notion of stepwise addition and deletion of knots in this context.

Stepwise addition. The most natural way to proceed from one step to the next in the stepwise addition procedure is to introduce a new vertex into the existing triangulation, thereby adding one new basis function to the existing spline space. This operation requires a rule for connecting this point to the vertices in Δ so that the new mesh is also a conforming triangulation. In Figure 15, we illustrate three options for vertex addition: we can place a new vertex on either a boundary or an interior edge, splitting the edge, or we can add a point to the interior of one of the triangles in Δ . Note that the space obtained by adding a vertex \mathbf{v} to an interior edge of a triangle $\delta \in \Delta$ cannot be achieved as the limit of spaces constructed by adding \mathbf{v} to the interior of δ . In this case, if \mathbf{v} is very close to an edge of δ , the new triangulation is essentially nonconforming and the associated space of linear functions G contains elements that are discontinuous along that edge. Similar discontinuities arise when the new point \mathbf{v} is positioned extremely close to an existing vertex. Degeneracies such as these are encountered in the context of univariate spline spaces when knots are allowed to coalesce [de Boor (1978)].

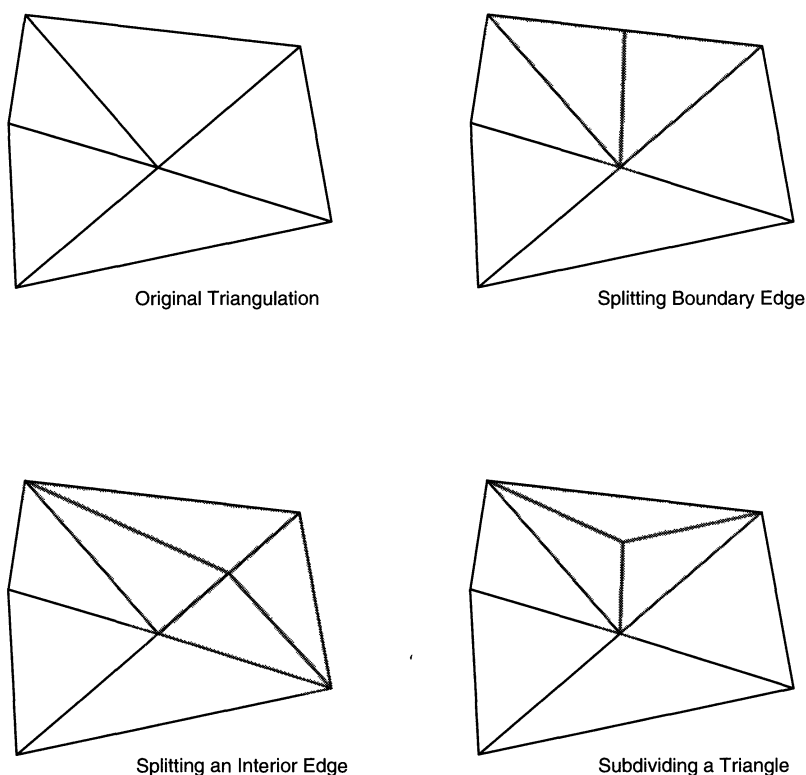


FIG. 15. Three ways to add a new vertex to an existing triangulation. Each addition represents the introduction of a single basis function, the support of which is colored gray.

Given a triangulation Δ , we construct a set of candidate vertices by considering the points with barycentric coordinates

$$(9.4) \quad \left(\frac{k_1}{K+1}, \frac{k_2}{K+1}, \frac{K+1-k_1-k_2}{K+1} \right)_\delta, \quad \delta \in \Delta,$$

where k_1 , k_2 and K are nonnegative integers satisfying $k_1 + k_2 \leq K + 1$ and no coordinate equals 1. We have introduced a subscript δ to make it clear that these points are calculated for each triangle in Δ . At each step in the addition process, we select from this set of candidate vertices the point that maximizes the Rao statistic described in Section 3. Stability considerations may dictate that we do not consider for addition vertices in areas where there is little data. Moreover, we have found it useful to avoid creating triangles having one or two very small angles. Restrictions such as these are easily incorporated into the stepwise addition procedure.

Stepwise deletion. There are two possible strategies for reducing the dimension of an existing piecewise linear spline space. In each case, we enforce the condition that a function in the space be continuously differentiable across a given edge in the existing triangulation. Observe that a continuous, piecewise linear function has continuous partial derivatives across an edge if and only if the function is linear on the union of the two triangles that share the edge. Using the correspondence between vertices and basis functions described above, we can show that the subspace of spline functions satisfying this condition is characterized by a simple linear constraint of the type discussed in Section 3. In each of the examples in Figure 15, enforcing continuity of the first partial derivatives across any of the gray edges is equivalent to removing the added vertex, returning us to the original partition in the upper left corner of the figure. Thus, in light of the stepwise knot deletion strategy discussed in the previous sections, one procedure for stepwise deletion in the bivariate context involves using the Wald statistic to choose between continuity constraints across edges that fall into one of the three categories listed in Figure 15. An alternative deletion procedure is somewhat more aggressive and involves choosing from among all the continuity constraints, regardless of how the edge is positioned relative to the other edges in the partition. The important distinction between these two procedures is that only in the first case are we actually guaranteed that the structure of Δ is simplified at each step.

9.3. Bivariate logspline density estimation.

Maximum likelihood estimation. While the bivariate methodology introduced in the previous paragraphs has been implemented for a variety of extended linear models, we will focus mainly on logspline density estimation. In this context, we choose to model the logarithm of an unknown density ϕ of a random vector \mathbf{U} as a bivariate spline. For ease of presentation, we restrict our attention to densities that are supported on a simply connected region $\mathcal{U} \in \mathbb{R}^2$ having a polygonal boundary. As usual, let Δ denote a conforming partition of

\mathcal{U} and let $B_1(\mathbf{u}), \dots, B_J(\mathbf{u})$ denote the basis functions of the corresponding space G of continuous, piecewise linear functions over Δ .

Given a vector $\boldsymbol{\beta} = (\beta_1, \dots, \beta_J) \in \mathbb{R}^J$, we can define a density $f(\mathbf{u}; \boldsymbol{\beta})$ over \mathcal{U} having the form

$$f(\mathbf{u}; \boldsymbol{\beta}) = \exp(\beta_1 B_1(\mathbf{u}) + \dots + \beta_J B_J(\mathbf{u}) - C(\boldsymbol{\beta})),$$

where

$$C(\boldsymbol{\beta}) = \log \int_{\mathcal{U}} \exp(\beta_1 B_1(\mathbf{u}) + \dots + \beta_J B_J(\mathbf{u})) \, d\mathbf{u}$$

is the normalizing constant. Based on a random sample $\mathbf{U}_1, \dots, \mathbf{U}_n$ from the distribution of \mathbf{U} , we estimate ϕ by the function $\hat{\phi} = f(\mathbf{u}; \hat{\boldsymbol{\beta}})$, where $\hat{\boldsymbol{\beta}}$ maximizes the “log-likelihood” $l(\boldsymbol{\beta}) = \log f(\mathbf{U}_1; \boldsymbol{\beta}) + \dots + \log f(\mathbf{U}_n; \boldsymbol{\beta})$. While we do not believe that $l(\cdot)$ is the true log-likelihood function corresponding to our sample, we know from the discussion at the beginning of this section that as $n \rightarrow \infty$, $\hat{\phi}$ tends to ϕ .

As in univariate logspline density estimation (see Section 4), the likelihood equations take on the very simple form

$$(9.5) \quad E_{\boldsymbol{\beta}} B_j(\mathbf{U}) = E_n B_j(\mathbf{U}), \quad 1 \leq j \leq J,$$

where

$$E_{\boldsymbol{\beta}} B_j(\mathbf{U}) = \int_{\mathcal{U}} B_j(\mathbf{u}) f(\mathbf{u}; \boldsymbol{\beta}) \, d\mathbf{u} \quad \text{and} \quad E_n B_j(\mathbf{U}) = \frac{1}{n} \sum_{i=1}^n B_j(\mathbf{U}_i).$$

Since the functions B_j are piecewise linear over \mathcal{U} , it is possible to evaluate the required integrals exactly. As in previous sections, the equations in (9.5) are solved using Newton–Raphson iterations. To obtain the Hessian matrix required for this procedure, we must also calculate expressions of the form $E_{\boldsymbol{\beta}}[B_{j_1}(\mathbf{U})B_{j_2}(\mathbf{U})]$ for $1 \leq j_1, j_2 \leq J$. Since the basis functions are piecewise linear, however, we again do not require numerical quadrature to carry out these computations.

Implementing stepwise addition and deletion. Recall that we add basis functions to G by adding vertices to Δ and that our strategy for choosing between the competing basis functions is based on the heuristic maximization of Rao statistics. This process can be simplified considerably by making explicit use of the barycentric coordinate functions discussed above. For example, suppose that we want to add a node \mathbf{v} inside δ , the right-hand triangle in Figure 16. Once again, suppose that δ has vertices $\mathbf{v}_1, \mathbf{v}_2$ and \mathbf{v}_3 and let $\varphi_1(\mathbf{u}), \varphi_2(\mathbf{u})$ and $\varphi_3(\mathbf{u})$ denote the barycentric coordinates of a point $\mathbf{u} \in \mathbb{R}^2$ relative to δ . Now, if we let $B_1(\mathbf{u}), B_2(\mathbf{u})$ and $B_3(\mathbf{u})$ represent the piecewise linear basis functions associated with the points $\mathbf{v}_1, \mathbf{v}_2$ and \mathbf{v} in the updated triangulation, then it is straightforward to demonstrate that, for all points \mathbf{u} in the shaded triangle on the right in Figure 16,

$$\begin{aligned} \varphi_1(\mathbf{u}) &= B_1(\mathbf{u}) + \varphi_1(\mathbf{v})B_3(\mathbf{u}), & \varphi_2(\mathbf{u}) &= B_2(\mathbf{u}) + \varphi_2(\mathbf{v})B_3(\mathbf{u}) \quad \text{and} \\ \varphi_3(\mathbf{u}) &= \varphi_3(\mathbf{v})B_3(\mathbf{u}). \end{aligned}$$

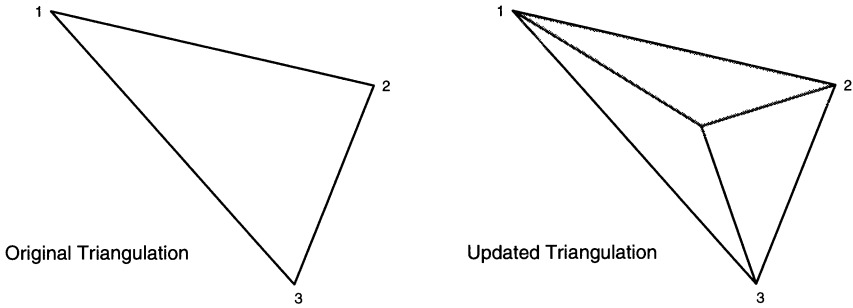


FIG. 16. Adding a new vertex at the point $\mathbf{v} = \varphi_1(\mathbf{v})\mathbf{v}_1 + \varphi_2(\mathbf{v})\mathbf{v}_2 + \varphi_3(\mathbf{v})\mathbf{v}_3$. In this case, we are adding to G the continuous, piecewise linear function that takes on the value 1 at the point \mathbf{v} and 0 at each of \mathbf{v}_1 , \mathbf{v}_2 and \mathbf{v}_3 .

Combining these relationships with the fact that within δ , the piecewise linear basis functions associated with \mathbf{v}_1 , \mathbf{v}_2 and \mathbf{v}_3 are exactly the barycentric coordinate functions relative to δ , we arrive at simple formulas for calculating the necessary inner products and empirical moments that go into forming the Rao statistic for adding \mathbf{v} to the partition Δ . Similar expressions can be derived for evaluating the candidate function over the remaining two triangles in the right plot of Figure 16. In the numerical example discussed below, we introduce vertices at the points corresponding to $K = 5$ in expression (9.4).

Using these ideas, we can also derive a simple procedure for determining the constraint that a function in G be continuously differentiable across a given edge in Δ . To make this more precise, consider the triangulation on the left in Figure 17 and let $\varphi_1(\mathbf{u})$, $\varphi_2(\mathbf{u})$ and $\varphi_3(\mathbf{u})$ denote the barycentric coordinates of a point $\mathbf{u} \in \mathbb{R}^2$ relative to the triangle with vertices \mathbf{v}_1 , \mathbf{v}_2 and \mathbf{v}_3 . Given a function $g \in G$, let β_1 , β_2 and β_3 denote the coefficients of the basis functions associated with these vertices. Then for all points \mathbf{u} in this triangle, $g(\mathbf{u})$ is the linear function given by $\beta_1\varphi_1(\mathbf{u}) + \beta_2\varphi_2(\mathbf{u}) + \beta_3\varphi_3(\mathbf{u})$. Now, if we let β_4 denote the coefficient of the basis function of G associated with the vertex \mathbf{v}_4 , then $g(\mathbf{v}_4) = \beta_4$. Therefore, the function g is linear on the

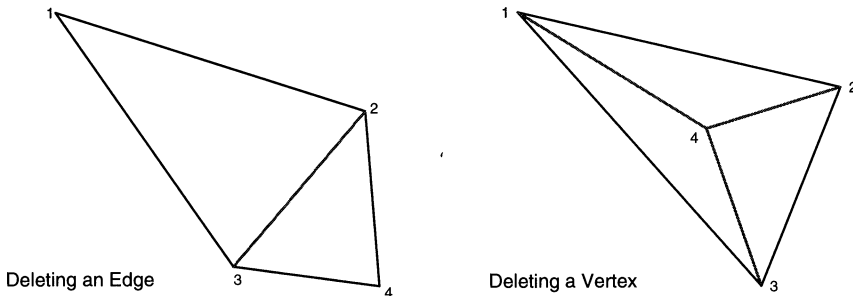


FIG. 17. The effect of enforcing the constraint that functions in G be continuously differentiable across edges in two triangulations.

union of the two triangles in the left portion of Figure 17 provided that

$$\beta_4 = g(\mathbf{v}_4) = \beta_1\varphi_1(\mathbf{v}_4) + \beta_2\varphi_2(\mathbf{v}_4) + \beta_3\varphi_3(\mathbf{v}_4).$$

By swapping the roles of \mathbf{v}_1 and \mathbf{v}_4 in this argument, we find that C^1 continuity of a function $g \in G$ can also be assured by the constraint

$$\beta_1 = g(\mathbf{v}_1) = \beta_2\tilde{\varphi}_2(\mathbf{v}_1) + \beta_3\tilde{\varphi}_3(\mathbf{v}_1) + \beta_4\tilde{\varphi}_4(\mathbf{v}_1),$$

where $\tilde{\varphi}_2(\mathbf{u})$, $\tilde{\varphi}_3(\mathbf{u})$ and $\tilde{\varphi}_4(\mathbf{u})$ denote the barycentric coordinates of a point \mathbf{u} relative to the triangle with vertices \mathbf{v}_2 , \mathbf{v}_3 and \mathbf{v}_4 . It is not hard to demonstrate that these two constraints are equivalent up to a multiplicative constant. Observe, however, that when this condition is enforced, we are left with a single linear function over the pair of triangles that constitute Δ , but we have not produced a simpler triangulation in the process.

Suppose instead that we want to remove the vertex \mathbf{v}_4 in the middle of the triangle in the right portion of Figure 17. Given $g \in G$ and $1 \leq i \leq 4$, we again let β_i correspond to the coefficient of the basis function associated with the vertex \mathbf{v}_i . It can be shown that each of the C^1 continuity constraints across the shaded interior edges shown in the figure is of the form

$$(9.6) \quad \beta_4 = \varphi_1(\mathbf{v}_4)\beta_1 + \varphi_2(\mathbf{v}_4)\beta_2 + \varphi_3(\mathbf{v}_4)\beta_3,$$

where $\varphi_1(\mathbf{u})$, $\varphi_2(\mathbf{u})$ and $\varphi_3(\mathbf{u})$ are the barycentric coordinates of a point \mathbf{u} relative to the outer triangle in Figure 17. Observe that the expression on the left is the value at \mathbf{v}_4 of the unique linear function interpolating β_1 , β_2 and β_3 at the points \mathbf{v}_1 , \mathbf{v}_2 and \mathbf{v}_3 , respectively. Recalling that $g(\mathbf{v}_4) = \beta_4$, we see that the constraint in (9.6) has considerable intuitive appeal.

9.4. An example. We end our discussion of bivariate logspline density estimation with an example suggested to us by Karl Broman. The points in the left panel of Figure 18 represent a collection of amino acids obtained from 100 protein structures taken from the Brookhaven Protein Data Bank [see Hobohm, Scharf, Schneider and Sander (1992)]. In order to characterize the *local environment* of each amino acid within a given protein structure, three pieces of information were recorded: the local structure of the protein at the given amino acid (whether the protein is twisting around a helix, for example), the fraction of the amino acid side-chain area that is buried in the protein structure and the fraction of the side-chain area that is covered by polar atoms. Because the unburied portion of the amino acid is exposed to a polar solvent, the final two quantities are restricted to the upper triangle of the unit square. In Figure 18, for example, we plot these two measurements for all of the occurrences of the amino acid lysine for which the local protein structure is a helix.

Bivariate density estimates computed for each amino acid and each local protein structure are the basis for an approach to solving the so-called inverse folding problem [see Bowie, Luthy and Eisenberg (1991) and Zhang and Eisenberg (1994)]. Evaluating the structure of a given protein is extremely difficult. Determining the sequence of amino acids that comprise the protein,

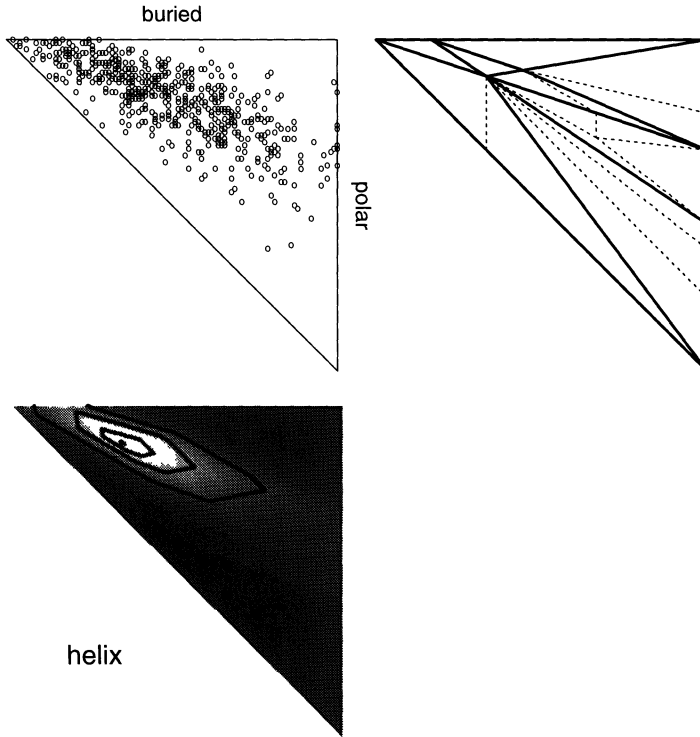


FIG. 18. *Applying the density estimation routine. In the top row we present the data and both the triangulation obtained from stepwise addition (thin, dashed line) and that obtained from stepwise deletion (thick, solid line). In the bottom row we present the data along with a contour plot of the final fit from the deletion process.*

however, is relatively simple. It would seem reasonable, therefore, to attempt to infer the protein's structure from its amino acid sequence. Unfortunately, many rather different sequences produce very similar structures, so the objective of the inverse folding problem is to determine which amino acid sequences might result in a given known structure. This can be accomplished by studying the propensity for certain amino acids to occur in certain local environments in a large collection of known protein structures. The procedure described by Zhang and Eisenberg involves a log-odds calculation, the main ingredient of which is a set of bivariate density estimates for the type of data given in Figure 18.

In the bottom panel of Figure 18, we present a contour plot of the density estimate obtained by stepwise addition followed by stepwise deletion. The model shown was encountered during stepwise deletion and attains the minimum BIC value among all the models obtained during both the stepwise addition and deletion processes. During this process, we selected candidate knots corresponding to $K = 5$ in (9.4), and did not consider any new vertices that would result in a triangle containing fewer than 25 points. In the panel on the upper

right in the same figure, we present the final triangulation along with dashed edges to indicate the additional structure present when the stepwise deletion process began. The fits as well as the various plots in Figure 18 were produced using a library of S/S-PLUS routines that are available from Hansen.

In this section we have introduced a method for bivariate density estimation using piecewise linear, bivariate splines based on an adaptively constructed triangulation. We have also implemented this procedure for both regression and generalized regression. The resulting estimates, which we have named Triograms, have performed well on a variety of bivariate data sets taken from a number of different estimation contexts. The interested reader is referred to Hansen, Kooperberg and Sardy (1996), where Triograms are compared to several existing function estimation routines. One advantage that Triograms have over these other methods is that the entire estimation procedure is invariant under affine transformations and is the most natural approach for modeling data when the domain of the predictor variables is a polygonal region in the plane. As anticipated by the convergence rate derived at the beginning of this section, if our underlying function ϕ is smooth, piecewise linear estimates are suboptimal. This problem can be corrected by using higher-order splines, and we are currently investigating how to extend the Triogram procedure to make use of the generalized vertex splines of Chui and He (1990).

REFERENCES

- ANDERSEN, P. K., BORGAN, Ø., GILL, R. D. and KEIDING, N. (1993). *Statistical Models Based on Counting Processes*. Springer, New York.
- BELSEY, D. A., KUH, E. and WELSCH, R. E. (1980). *Regression Diagnostics: Identifying Influential Data and Sources of Collinearity*. Wiley, New York.
- BOURLARD, H. A. and MORGAN, N. (1994). *Connectionist Speech Recognition*. Kluwer, Boston.
- BOWIE, J. U., LUTHY, R. and EISENBERG, D. (1991). A method to identify protein sequences that fold into a known 3-dimensional structure. *Science* **253** 164–170.
- BREIMAN, L. (1993). Fitting additive models to regression data. *Comput. Statist. Data Anal.* **15** 13–46.
- BREIMAN, L., FRIEDMAN, J. H., OLSHEN, R. A. and STONE, C. J. (1984). *Classification and Regression Trees*. Wadsworth, Belmont, CA.
- BRESLOW, N. E. (1972). Contribution to the discussion on the paper by D. R. Cox, Regression and life tables. *J. Roy. Statist. Soc. Ser. B* **34** 216–217.
- BRESLOW, N. E. (1974). Covariance analysis of censored survival data. *Biometrics* **30** 89–99.
- BRILLINGER, D. R. (1981). *Time Series: Data Analysis and Theory*. Holden-Day, San Francisco.
- CHUI, C. K. (1988). *Multivariate Splines*. SIAM, Philadelphia.
- CHUI, C. K. and HE, T. (1990). Bivariate C^1 quadratic finite elements and vertex splines. *Math. Comp.* **54** 169–187.
- COLE, R., NOEL, M., BURNETT, D. C., FANTY, M., LANDER, T., OSHIKA, B. and SUTTON, S. (1994). Corpus development activities at the Center for Spoken Language Understanding. Technical report, CSLU, Portland, OR.
- COLE, R. A., ROGINSKI, K. and FANTY, M. (1992). A telephone speech database of spelled and spoken names. In *Proceedings of the International Conference on Spoken Language Processing* 891–893. Quality Color Press, Univ. Alberta, Edmonton.
- COX, D. R. (1972). Regression models and life tables (with discussion). *J. Roy. Statist. Soc. Ser. B* **34** 187–220.
- COX, D. R. and OAKES, D. (1984). *Analysis of Survival Data*. Chapman and Hall, London.
- DE BOOR, C. (1978). *A Practical Guide to Splines*. Springer, New York.

- DE BOOR, C. (1987). B-form basics. In *Geometric Modeling* (G. Farin, ed.) 131–148. SIAM, Philadelphia.
- DURKA, P. J., KELLY, E. F. and Blinowska, K. J. (1995). Time-frequency analysis of stimulus-driven EEG activity by matching pursuit. In *Proceedings of the 18th Annual Conference of the IEEE EMBS, Amsterdam, October 31–November 3, 1996*. IEEE, New York.
- FAMILY EXPENDITURE SURVEY (1968–1983). Annual base tapes and reports (1968–1983). Dept. Employment, Statistics Division, Her Majesty's Stationary Office, London.
- FAN, J. and GJJBELS, I. (1996). *Local Polynomial Modeling and Its Applications*. Chapman and Hall, London.
- FARIN, G. (1986). Triangular Bernstein–Bézier patches. *Comput. Aided Geom. Design* **3** 83–127.
- FLEMING, T. R. and HARRINGTON, D. P. (1991). *Counting Processes and Survival Analysis*. Wiley, New York.
- FRIEDMAN, J. H. (1991). Multivariate adaptive regression splines (with discussion). *Ann. Statist.* **19** 1–141.
- FRIEDMAN, J. H. and SILVERMAN, B. W. (1989). Flexible parsimonious smoothing and additive modeling (with discussion). *Technometrics* **31** 3–39.
- GAUVAIN, J. L., LAMEL, L. F., ADDA, G. and ADDA-DECKER, M. (1994). Speaker-independent continuous speech dictation. *Speech Communication* **15** 21–37.
- GRAY, R. J. (1992). Flexible methods for analyzing survival data using splines, with applications to breast cancer prognosis. *J. Amer. Statist. Assoc.* **87** 942–951.
- GREEN, P. J. and SILVERMAN, B. W. (1994). *Nonparametric Regression and Generalized Linear Models: A Roughness Penalty Approach*. Chapman and Hall, London.
- GU, G. and WAHBA, G. (1993). Smoothing spline ANOVA with component-wise Bayesian “confidence intervals.” *J. Comput. Graph. Statist.* **2** 97–117.
- HANSEN, M. (1994). Extended linear models, multivariate splines and ANOVA. Ph.D. dissertation, Dept. Statistics, Univ. California, Berkeley.
- HANSEN, M., KOOPERBERG, C. and SARDY, S. (1996). Triograms models. *J. Amer. Statist. Assoc.* To appear.
- HASTIE, T. and TIBSHIRANI, R. (1990). *Generalized Additive Models*. Chapman and Hall, London.
- HERMANSKY, H. (1990). Perceptual linear predictive (PLP) analysis of speech. *Journal of the Acoustical Society of America* **87** 1738–1752.
- HOBOHM, U., SCHARF, M., SCHNEIDER, R. and SANDER, C. (1992). Selection of representative protein data sets. *Protein Science* **1** 409–417.
- KALBFLEISCH, J. D. and PRENTICE, R. L. (1980). *The Statistical Analysis of Failure Time Data*. Wiley, New York.
- KAPLAN, E. L. and MEIER, P. (1958). Nonparametric estimation from incomplete observations. *J. Amer. Statist. Assoc.* **53** 457–481.
- KENNEDY, W. J. and GENTLE, J. E. (1980). *Statistical Computing*. Dekker, New York.
- KOOPERBERG, C., BOSE, S. and STONE, C. J. (1997). Polychotomous regression. *J. Amer. Statist. Assoc.* **92** 117–127.
- KOOPERBERG, C. and STONE, C. J. (1991). A study of logspline density estimation. *Comput. Statist. Data Anal.* **12** 327–347.
- KOOPERBERG, C. and STONE, C. J. (1992). Logspline density estimation for censored data. *J. Comput. Graph. Statist.* **1** 301–328.
- KOOPERBERG, C., STONE, C. J. and TRUONG, Y. K. (1995a). Hazard regression. *J. Amer. Statist. Assoc.* **90** 78–94.
- KOOPERBERG, C., STONE, C. J. and TRUONG, Y. K. (1995b). The L_2 rate of convergence for hazard regression. *Scand. J. Statist.* **22** 143–157.
- KOOPERBERG, C., STONE, C. J. and TRUONG, Y. K. (1995c). Logspline estimation of a possibly mixed spectral distribution. *J. Time Ser. Anal.* **16** 359–388.
- KOOPERBERG, C., STONE, C. J. and TRUONG, Y. K. (1995d). Rate of convergence for logspline spectral density estimation. *J. Time Ser. Anal.* **16** 389–401.
- MCCULLAGH, P. and NELDER, J. A. (1989). *Generalized Linear Models*, 2nd ed. Chapman and Hall, London.
- MILLER, R. G. (1981). *Survival Analysis*. Wiley, New York.
- PARZEN, E. (1979). Nonparametric statistical data modeling. *J. Amer. Statist. Assoc.* **74** 105–131.

- RABINER, L. and JUANG, B.-H. (1993). *Fundamentals of Speech Recognition*. Prentice-Hall, Englewood Cliffs, NJ.
- SCHWARZ, G. (1978). Estimating the dimension of a model. *Ann. Statist.* **6** 461–464.
- SILVERMAN, B.W. (1986). *Density Estimation for Statistics and Data Analysis*. Chapman and Hall, London.
- SLEEPER, L. A. and HARRINGTON, D. P. (1990). Regression splines in the Cox model with application to covariate effects in liver disease. *J. Amer. Statist. Assoc.* **85** 941–949.
- SMITH, P. L. (1982). Curve fitting and modeling with splines using statistical variable selection techniques. Report NASA 166034, NASA, Langley Research Center, Hampton, VA.
- SOLVD INVESTIGATORS (1990). Studies of left ventricular dysfunction (SOLVD)—rationale, design, and methods: two trials that evaluate the effect of enalapril in patients with reduced ejection fraction. *American Journal of Cardiology* **6** 315–322.
- STONE, C. J. (1985). Additive regression and other nonparametric models. *Ann. Statist.* **13** 689–705.
- STONE, C. J. (1986). The dimensionality reduction principle for generalized additive models. *Ann. Statist.* **14** 590–606.
- STONE, C. J. (1990). Large-sample inference for log-spline models. *Ann. Statist.* **18** 717–741.
- STONE, C. J. (1991). Asymptotics for doubly flexible logspline response models. *Ann. Statist.* **19** 1832–1854.
- STONE, C. J. (1994). The use of polynomial splines and their tensor products in multivariate function estimation (with discussion). *Ann. Statist.* **22** 118–184.
- STONE, C. J. and KOO, C.-Y. (1986a). Additive splines in statistics. In *Proceedings of the Statistical Computing Section* 45–48. Amer. Statist. Assoc., Alexandria, VA.
- STONE, C. J. and KOO, C.-Y. (1986b). Logspline density estimation. *Contemp. Math.* **59** 1–15.
- WAHBA, G. (1990). *Spline Models for Observational Data*. SIAM, Philadelphia.
- WAND, M. P. and JONES, M. C. (1995). *Kernel Smoothing*. Chapman and Hall, London.
- WAND, M. P., MARRON, S. J. and RUPPERT, D. (1991). Transformations in density estimation (with discussion). *J. Amer. Statist. Assoc.* **86** 343–361.
- ZHANG, K. and EISENBERG, D. (1994). The three-dimensional profile method using residue preference as a continuous function of residue environment. *Protein Science* **3** 687–695.

CHARLES J. STONE
DEPARTMENT OF STATISTICS
UNIVERSITY OF CALIFORNIA
BERKELEY, CALIFORNIA 94720-3860
E-MAIL: stone@stat.berkeley.edu

MARK H. HANSEN
BELL LABORATORIES
700 MOUNTAIN AVE., RM. 2C260
MURRAY HILL, NEW JERSEY 07030

CHARLES KOOPERBERG
FRED HUTCHINSON CANCER RESEARCH CENTER
1100 FAIRVIEW AVE., MP 1002
SEATTLE, WASHINGTON 98109-1024

YOUNG K. TRUONG
DEPARTMENT OF BIostatISTICS
UNIVERSITY OF NORTH CAROLINA
CHAPEL HILL, NORTH CAROLINA 27599-7400
E-MAIL: truong@stat.unc.edu

DISCUSSION

JIANQING FAN

*University of North Carolina, Chapel Hill
and Chinese University of Hong Kong*

I would like to congratulate Stone, Hansen, Kooperberg and Truong for successfully outlining an ingenious principle on flexible statistical modeling. This principle is convincingly and successfully applied to a wide array of statistical